Integrated approach for the development across Europe of user oriented climate indicators for GFCS high-priority sectors: Agriculture, disaster risk reduction, energy, health, water and tourism

Work Package 4

Deliverable 4.4

INDECIS-ISD released and integrated into de IDISP

Fernando Domínguez-Castro[1,2], Dhais Peña-Angulo[3], Jesús Revuelto[3], Fergus Reig[3], Sergio M. Vicente-Serrano[3], Enric Aguilar[4], Iván Noguera[3], Gerard van der Schrier[5], Ahmed M. El Kenawy[6,7]

[1]ARAID Foundation, Zaragoza, 50018, Spain
[2]Departamento de Geografía y Ordenación del Territorio, Universidad de Zaragoza, Zaragoza, 50009, Spain
[3]Instituto Pirenaico de Ecología, Consejo Superior de Investigaciones Científicas (IPE–CSIC), Zaragoza, 50059, Spain,
[4]Center for Climate Change, Universitat Rovira i Virgili, Tarragona, 43480, Spain
[5]Royal Netherlands Meteorological Institute (KNMI), 3730 AE, De Bilt, Netherlands.
[6]Department of Geography, Sultan Qaboos University, Al Khoud, Muscat, 123, Oman
[7]Department of Geography, Mansoura University, Mansoura, 35516, Egypt

This report arises from the Project INDECIS which is part of ERA4CS, an ERA-NET initiated by JPI Climate, and funded by FORMAS (SE), DLR (DE), BMWFW (AT), IFD (DK), MINECO (ES), ANR (FR), with co-funding by the European Union's Horizon 2020 research and innovation programme

Table of Contents

1

Overview

This deliverable describes the latest analysis of the climate indices calculated in the frame of INDECIS European project. In total, 125 standard climate indices spanning in two distinct time periods, 1950-2017 and 1979-2017 and distributed for the whole Europe with a 0.25º grid cell size have been calculated. This database allows a deeper understanding of recent climate evolution, with important implications for different sectors and socioeconomic activities, mainly focusing on water resources, health, energy, tourism and agriculture. Here it is firstly described a multidecadal assessment on these climatic indices computed at different temporal scales and secondly it is detailed a new dataset of four statistical parameters (climatology, coefficient of variation, slope and significant trend) of the 125 indices.

Evaluating the spatio-temporal evolution of climate processes is highly complex due to the large number of interrelated processes taking place simultaneously in the climatic system. Thereby, to understand and assess the evolution of the climatic system; requires high quality databases of standard climate metrics computed in different time periods and distributed over extended areas, which spams over long time periods. Nowadays, different dataset provide updated variables in a daily basis of distinct variables, including air temperature, precipitation, sea level pressure, wind, total cloud cover insolation or snow depth among others. INDECIS project has exploited two dataset to compute the 125 indices, the European Climate Assesment & Dataset (ECA&D)E-OBS and the ERA-5 re-analysis. These dataset have been exploited to compute a gridded dataset at different temporal scales for the whole Europe. The main characteristics of this multidecadal dataset of climate indices are described here.

Similarly, analysing the trend that the climatic system shows at different spatial and temporal scales requires detailed databases of climatic parameters. In view of this necessity, it has been computed the "European Climatology and Trend Atlas of Climate Indices" (ECTACI), containing different climate parameters for the European region. This new atlas is available for the period 1979-2017 in monthly, seasonal and annual time scales, for the 125 INDECIS standard indices and thus with same spatial resolution. This deliverable includes a detailed description of the atlas and also the general trends of different climate indices at seasonal and annual scales for Europe. This information is highly valuable for understanding the existent link between the climatic evolution and changes occurring in different socio-economic sectors in the last 40 years.

A multidecadal assessment of climate indices over Europe

2.1 Abstract

Monitoring and management of several environmental and socioeconomic sectors requires climate data that can be summarized using a set of standard and meaningful climate metrics. Albeit with the availability of several climate datasets at the daily scale for Europe, none of these datasets deployed this information to create a dataset of climate indices and make it freely available for a wide range of end-users and sectorial applications (e.g. agriculture, insurance, health, energy production, etc.). In an attempt to fill such a knowledge gap, this study describes a newly developed gridded dataset for the whole Europe, which employed a set of 125 climate indices spanning the period from 1950 and updated yearly. This dataset comprehensively summarizes climate variability in Europe for a wide range of climate variables and conditions, including air temperature, precipitation, biometeorology, aridity, continentality, drought, amongst others. Climate indices were computed at different temporal scales (i.e. monthly, seasonal and annual) and mapped at a grid interval of 0.25º. This dataset is publicly available to research and end-users communities.

2.2 Background & Summary

Climate processes are usually very complex to be monitored and quantified. There is high degree of subjectivity when climate conditions determining environmental and societal impacts are quantified[1–3]. Although climate observations usually correspond to quantitative variables with a comprehensible physical meaning, the environmental, societal and economic impacts, including a number of sectors, usually depend on specific climate conditions or event characteristics[4–7]. For example, the cumulative climate conditions over long periods, the extreme values recorded over a period, the frequency of days with specific characteristics, the frequency of events above or below specific thresholds; amongst others, could have a direct influence on environmental and socioeconomic systems[8–11]. In the same context, monitoring and assessing the impact of climate is a complicated process, given that conditions that trigger specific impacts are often a result of interactions between different climate covariates. For example, bioclimatic conditions that strongly determine human health and comfort depend on a wide range of climate variables, such as air temperature, relative humidity, wind speed, etc.[12,13] Similarly, while drought severity is mainly controlled by precipitation, other climate variables (e.g. atmospheric evaporative demand, potential evaporation) could contribute significantly to drought dynamics[14–16].

Within this context, much effort has been made to develop synthetic climate indices, which can be employed to determine climate impacts on different natural systems and socioeconomic sectors[17–20]. These indices are also useful for providing a comprehensive assessment of climate variability and change processes under current and future climate change scenarios[21–24]. The joint Ccl/WCRP/JCOMM Expert Team on Climate Change Detection and Indices (ETCCDI)[25] developed an array of standard climate indices, which have widely been used to determine recent trends in climate conditions, with a particular focus on precipitation and temperature metrics. These indices have been widely used over different world regions such as Brazil[26], China[27,28], Africa[29,30], the Mediterranean[31,32], Indonesia[33], North America[34], central America[35], central Asia[36], amongst others. In addition, these indices have also been analysed to assess the consequences of projections for future climate change scenarios. For example, Aerenson et al.[37] have recently analyzed a suite of climate indices based on daily precipitation and temperature projections at the global scale, with the aim of determining possible future changes under 1.5ºC and 2ºC warming scenarios. This study indicated that temperature indices are likely to witness significant changes in the future. On the other hand, the behavior of precipitation indices is more complex and different scenarios may cause different changes in the intensity of precipitation. Other studies (e.g. Dong et al.[38]) employed climate indices to verify that the observed warming trends in Asia in the past six decades were inconsistent with the natural variability of the climate system but agreed with climate responses to external forcing as simulated by the models.

The availability of long-term, high spatial resolution and updated climate indices could be promising for the research community through a multidecadal assessment of climate change processes and their impacts. This climate information could also be useful for a wide variety of environmental and socioeconomic sectors (e.g. land and agricultural management, climate-based health impacts, insurance plans associated with weather extremes, etc). Currently, some climate indices datasets have been developed[34,39], mostly with the purpose of analyzing trends in climate conditions, focusing more on extreme meteorological events[40,41]. Nevertheless, in Europe there is not still an updated dataset of a wide variety of climate indices that can be useful for climate analysis and sectorial impact assessment. For this reason, the objective of this study is to provide an updated gridded dataset of a large variety of climate indices that summarize the temporal and spatial variability of climate in Europe during the past eight decades (from 1950 to 2017). Understanding climate services as "*The transformation of climate-related data – together with other relevant information – into customized products such as projections, forecasts, information, trends, economic analyses, assessments (including technology assessments), counselling on best practices, development and evaluation of solutions and any other service in relation to climate that may be of use for the society at large*"[42] *makes this dataset a potential assest from a climate service perspective. The target beneficiaries of this dataset may include climate services providers, civil society groups, farmers, amongst different stakeholders and end-users.*

2.3 Methods

Source datasets

To calculate the different climate indices, we employed two information sources: the European Climate Assessment & Dataset (ECA&D) E-OBS gridded dataset (https://www.ecad.eu/) and the ERA5 dataset (https://www.ecmwf.int/en/forecasts/datasets/reanalysis-datasets/era5). E-OBS dataset provides updated high quality daily air temperature, precipitation and sea level pressure data for Europe at different grid intervals from January 1950 onwards, with regular updates. This dataset was created from quality-controlled meteorological records[43], sourced from the European National Meteorological Services. Earlier versions of this dataset have been made available at a spatial resolution of 0.25º, being largly decreased their spatial reoltution in the recent versions of this product (0.1º and 0.25º for v17.0e). Herein, we produced our indices at a spatial resolution of 0.25º to be consistent with the resolution of ERA5. In pursuit of the ERA4CS INDECIS project (European Union Grant 690462), daily station data from ECA&D were homogenized[44] and the adjusted records will serve as a basis for the upcoming version of E-OBS datasets. The E-OBS dataset served as the main base for calculating climate indices related to air temperature and precipitation.

ERA5 is the last generation of the re-analysis dataset developed by the European Centre for Medium-Range Weather Forecasts (EWMF)[45]. Albeit with the availability of daily air temperature and precipitation data within ERA5, our preference was made to use ERA5 only to secure data for the climate variables not available in the observational datasets. This included data for dewpoint temperature at 2m, wind at 10m, wind gust at 10m, top-of-atmosphere (TOA) forcing, radiation, insolation, snow density, snow depth, snowfall, total cloud cover, and low cloud cover. Data from ERA5 were provided at a spatial resolution of 0.25º and hourly frequency. However, we aggregated the hourly data to daily scale to match the temporal resolution of E-OBS. To date, ERA5 is only available from February 1975; however, we will actualize the dataset for the early period (1950-1974) once data is available.

Figure 1 shows the spatial coverage of the study, our data set included the entire European continent, apart from Russia, Turkey and Cyprus. Our dataset comprises a total of 12280 series at a spatial resolution of 0.25º.

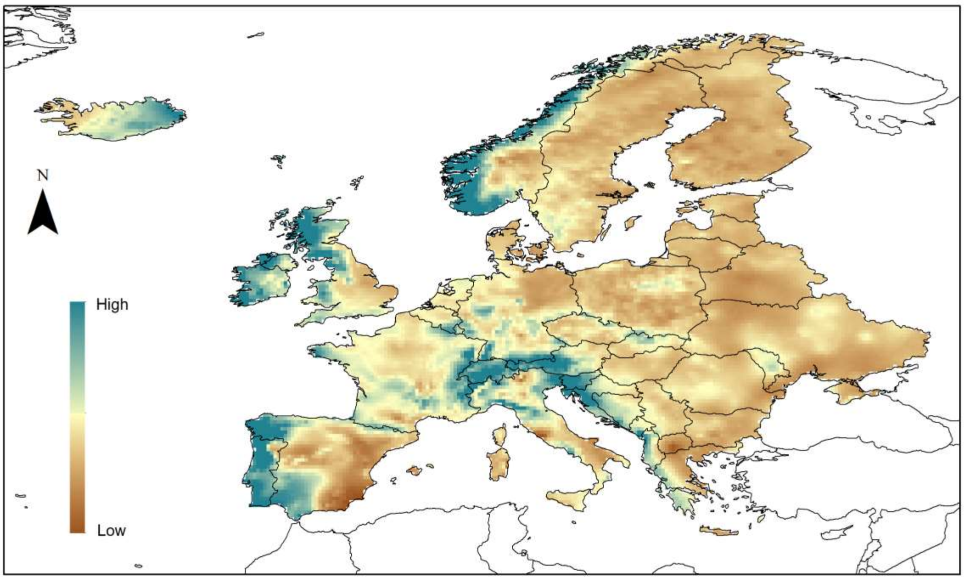

Figure 1: Spatial domain of the INDECISbase, the Modified Fournier Index is represented [MFI].

2.4 Index calculation

We calculated a set of 125 climate indices, based on a recently developed package (ClimInd) within R platform (ClimInd https://cran.r-project.org/web/packages/ClimInd/index.html). The climate indices were grouped into eight broad categories: i) temperature-based (N=42), ii) precipitation-based (N=21), iii) bioclimatic (N=21), iv) wind-based (N=5), v) aridity/continentality (N=10), vi) snow-based (N=12), vii) cloud/radiation-based (N=6), and viii) drought (N=8). Table 1 lists these indices and their description for the eight categories. The specific formulation of each index can also be consulted via: https://cran.r-project.org/web/packages/ClimInd/ClimInd.pdf. Overall, the majority of the indices were computed on monthly, seasonal (winter: DJF, spring: MAM, summer: JJA, autumn: SON) and annual scales. However, in some instances, specific indices were only calculated on the annual scale (e.g. the growing season precipitation [GSR], the modified Fournier index [MFI]). For those indices that require a base period for their calculation (e.g. percentile-based indices), we considered the entire period as a reference period. Herein, the 125 climate indices were computed for each one of the 12280 series covering the European continent.

Table 1: Climate indices contained in the database of INDECIS

Category	Name	Acronym
Temperature-based	Mean TX	GTX
	Maximum TX	XTX
	Minimum TX	NTX
	Mean TN	GTN
	Maximun TN	XTN
	Minimum TN	NTN
	Mean TG	GTG
	Maximum TG	XTG
	Minimum TG	NTG
	Cold days	TX10p
	Cold nights	TN10p
	Cold spell duration	CSDI
	Diurnal temperature range	DTR
	Mean daily difference DTR	vDTR
	Frost days	FD
	Growing season length	GSL
	Ice days	ID
	Maximum consecutive frost days	CFD
	Extreme temperature range	ETR
	Summer days	SU
	Maximum consecutive summer days	CSD
	Difference days above/below Tx17	DD17
	Tropical nights	TR
	Heating degree days	HD17
	Very cold days	VCD

	Very warm days	VWD
	Warm days	TX90p
	Warm nights	TN90p
	Warm spell duration	WSDI
	Zero crossing days	ZCD
	Onset of growing season 6 days	OGS6
	Onset of growing season 10 days	OGS10
	Growing season (Apr-Oct)	Ta_o
	Growing season(May-Sep)	Tm_s
	Growing degree days	GD4
	Winkler index	WKI
	Winter Severity	WS
	Sums TX32	STX32
	Days TX32	D32
	Sums TN-15	STN15
	Sums TN-10	STN10
	Sums positive	PTG
Precipitation-based	Total precipitation	Rt
	Maximun precipitation	RX1day
	Days precipitation ≥R10mm	R10mm
	Days precipitation ≥R20mm	R20mm
	Maximum 5 days R	Rx5day
	Simple daily intensity index	SDII
	Dry days	DD
	Effective precipitation	EP
	Longest dry period	CDD
	Longest wet period	CWD
	Precipitation fraction very wet days	R95tot
	Precipitation fraction extremely wet days	R99tot
	Heavy precipitation days	D50mm
	Very wet days	D95p
	Precipitation Concentration Index	PCI
	Modified Fournier Index	MFI
	Growing season precipitation	GSR
	Non-growing season precipitation	NGSR
	Total precipitation wet days	RTWD
	Wet days 1mm	DR1mm
	Wet days 3mm	DR3mm
Bioclimatic	TG warmest quarter	BIO10
	TG coldest quarter	BIO11
	Precipitation wettest month	BIO13
	Precipitation driest month	BIO14
	Coefficient of variation precipitation	BIO15
	Precipitation wettest quarter	BIO16

	Precipitation driest quarter	BIO17
	Precipitation warmest quarter	BIO18
	Precipitation coldest quarter	BIO19
	Temperature seasonality	BIO4
	TX warmest month	BIO5
	TN coldest month	BIO6
	Difference warmest/coldest month	BIO7
	TG wettest quarter	BIO8
	TG of driest quarter	BIO9
	Mean radiation	BIO20
	Universal thermal climate index	UTCI
	Mould index	MI
	Heat index	HI
	Wind chill index	WCI
	Apparent temperature	AT
wind-based	Days wind gusts above 21 m/s	DFx21
	Daily maximum wind gust	FXx
	Mean of daily mean wind strength	FG
	Calm days	fgcalm
	Days daily averaged wind above 10.8m/s	FG6Bft
aridity/continentality-indices	Reference evapotranspiration	ETo
	UNEP aridity index	UAI
	Climatic moisture deficit	CMD
	De Martonne aridity index	MAI
	Emberger aridity index	EAI
	Johansson Continentality Index	JCI
	Kerner Oceanity Index	KOI
	Pinna Combinative index	PiCI
	Budyko Index	BI
	Marsz Oceanity Index	MOI
snow-based	Snowfall sum	SS
	Snow days depth 1-10	SD0_10
	Snow days depth 10-20	SD10_20
	Frequency of snow days	FSD
	Mild snowy days	MSD
	Heavy snowy days	HSD
	Date of first snow cover	FSC
	Date of first permanent snow cover	FPSC
	Date of last permanent snow cover	LPSC
	Average snow depth	ASD
	Amount of snow covered days	SCD
	Maximum snow depth	MS
Cloud /radiation	Sum of sunshine duration	SSD
	Sunny days	SND

	Foggy days	FOD
	Mean daily cloud cover	CC
	Sunshine duration fraction	SSp
	Atmospheric Clarity Index	ACI
Drought	Standardized precipitation index 1	SPI1
	Standardized precipitation index 3	SPI3
	Standardized precipitation index 6	SPI6
	Standardized precipitation index 12	SPI12
	Standardised Precipitation-Evapotranspiration Index 1	SPEI1
	Standardised Precipitation-Evapotranspiration Index 3	SPEI3
	Standardised Precipitation-Evapotranspiration Index 6	SPEI6
	Standardised Precipitation-Evapotranspiration Index 12	SPEI12

Figure 2 illustrates the spatial variability of two selected indices (Rx1day and XTX) calculated on the annual scale for three specific years. Rx1day represents the maximum precipitation gauged within one day, whilst XTX refers to the highest daily maximum air temperature recorded during the year.

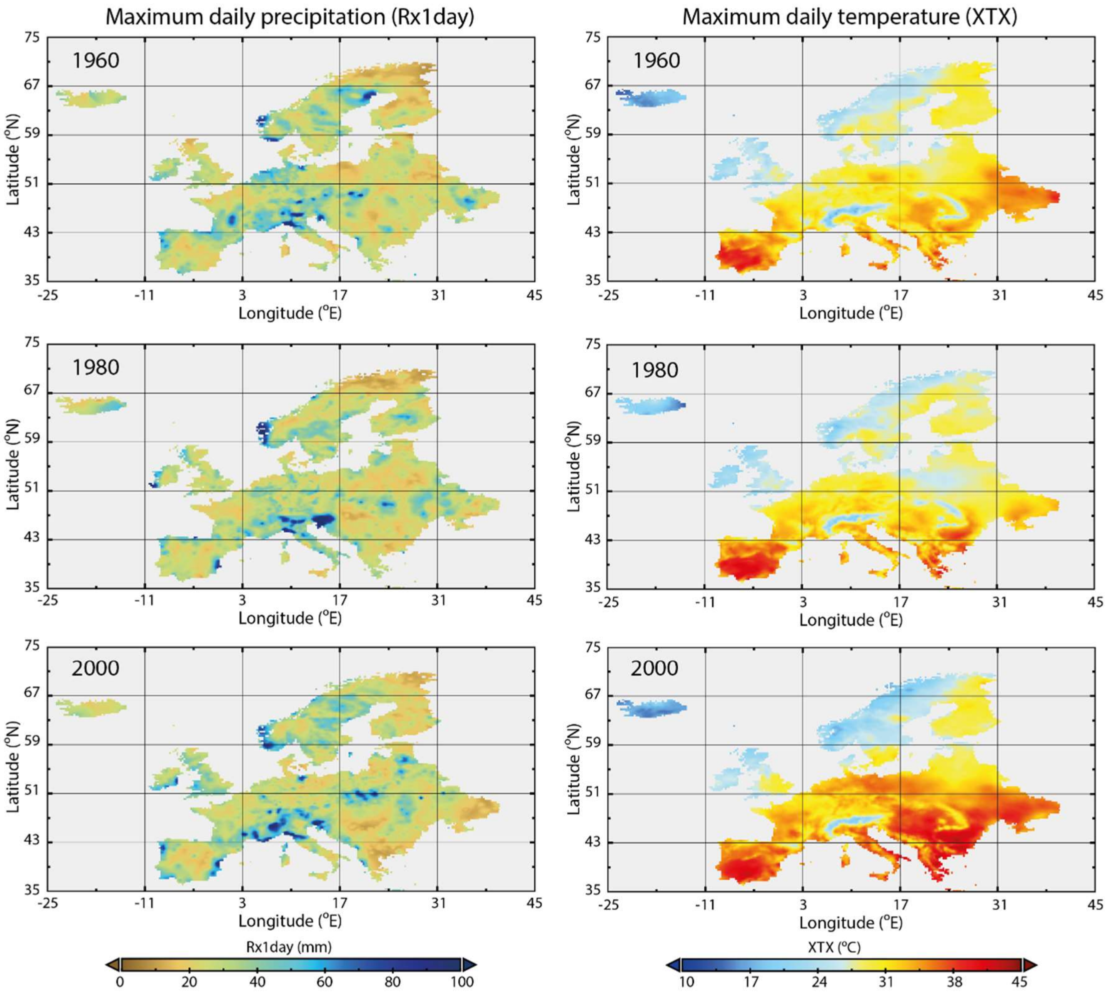

Figure 2: Spatial distribution of two of the climate indices (XTX and Rx1day) at the annual scale for three specific years (1960, 1980 and 2000).

Figure 3 depicts the temporal evolution of two selected climate indices (heavy precipitation days [D50mm] and the maximum consecutive frost days [CFD]) for ramdom selected grid points in Europe. The two indices were computed on the annual scale for the entire study period.

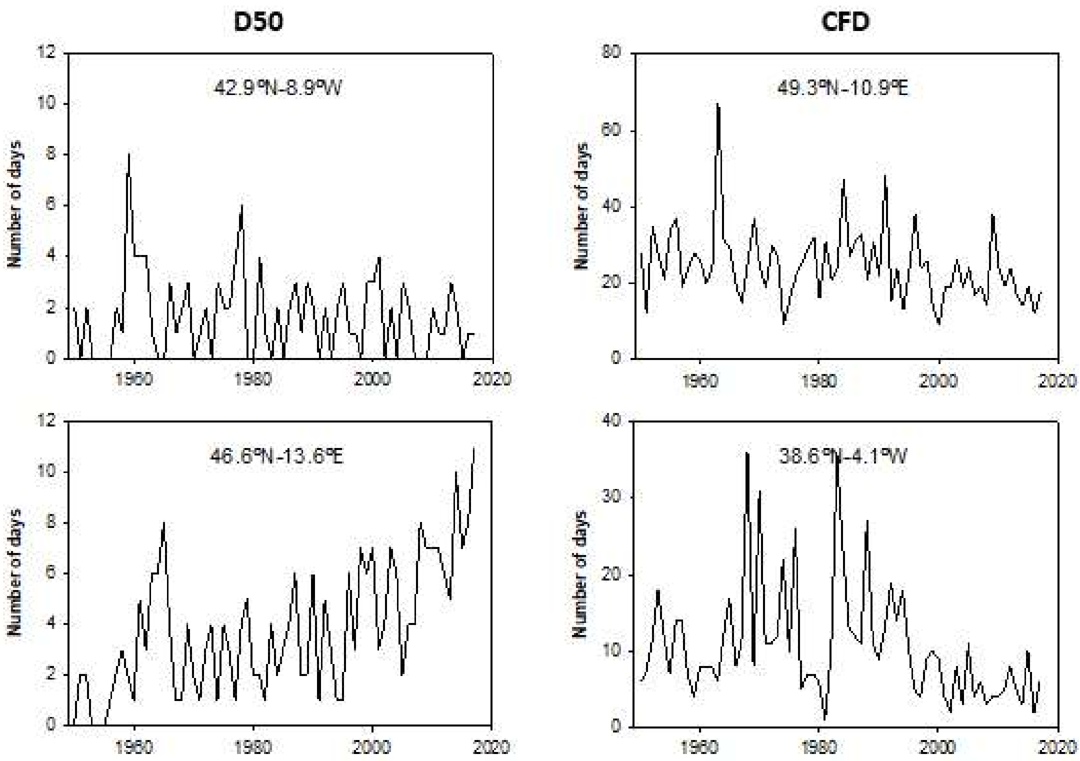

Figure 3: Temporal evolution of the annual D50mm and CFD indices calculated for specific grid points in Europe

2.5 Data records

The climate index dataset has been archived in figshare (https://figshare.com/), including all climate indices spanning the period 1950-2017. Given the high number of indices included in this dataset, we have stored the climate index data in different levels. The first level corresponds to the main index categories: temperature-based, precipitation-based, bioclimatic, wind-based, aridity/continentality, snow-based, cloud/radiation-based, and drought. Each of the first level categories (folders) is divided into subcategories (sub-folders); each of them corresponds to an individual climate index. Finally, at the third level, there are the data of each index at the different temporal scales availibles (i.e. monthly, seasonal and annual). The data were stored in a 3-D netcdf4 format (https://www.unidata.ucar.edu/software/netcdf/docs/netcdf_introduction.html). In specific, each file has an array of 464 (longitudes) x 201 (latitudes) x 68 (times for the annual resolution for the period 1950-2018). Indeed, the time dimension of the array varies as a function of the time resolution (i.e. monthly, seasonal, annual), as well as the period of time available (currently 1950 to 2017 for EOBS indices and 1979 to 2017 for ERA5 indices). The geographical extent of the dataset is 25.37ºN-75.37ºN and 40.37ºW-75.37ºE. Netcdf4 files can be visualized and manipulated with several types of software, including open source software like R, Panoply, etc., and Geographic Information System software (ArcGIS©, QGIS). A complete list of the available software can be found at https://www.unidata.ucar.edu/software/netcdf/software.html. The entire dataset comprises almost 1.000 million of data divided between the 125 indices and the different temporal scales (i.e. monthly, seasonal and annual).

2.6 Technical validation

The validation of our dataset depends largely on the reliability of climatic information used for calculating each index. The quality control and homogeneity of climatic data retrieved from the source datasets (i.e. E-OBS and ERA5) is comprehensively described in https://www.ecad.eu/download/ensembles/download.php for E-OBS and https://www.ecmwf.int/en/forecasts/datasets/reanalysis-datasets/era5 for ERA5. Technically, we assessed the performance of our developed R package (ClimInd) by checking the spatial and temporal consistency of the obtained climate indices. Also, the monthly, seasonal and annual values of the different indices were visually inspected to detect any possible problems.

2.7 Usage Notes

In addition to the stored dataset in the figshare repository, the climate indices are also available the project website (https://indecis.csic.es/), maintained by the Spanish National Research Council (Figure 4). In addition to its role as a data warehouse, the project's website can be used as a climate service, as end-users can select, visualize and download any index of interest for any grid point in Europe (Figure 5). These series can be downloaded in a generic ascii .txt format. The web site also allows navigation between the monthly, seasonal and annual archives and directly download any netcdf4 of the database. The entire dataset stored in this web site will be updated depending on the availability and updates of the ECA&D and ERA5 data, with at leasy yearly frequence. This website is mirrored at the INDECIS project portal (http://www.indecis.eu/indices.php).

Figure 4: Web-tool to visualize the INDECIS dataset and download the entire dataset corresponding to any spatial or temporal query.

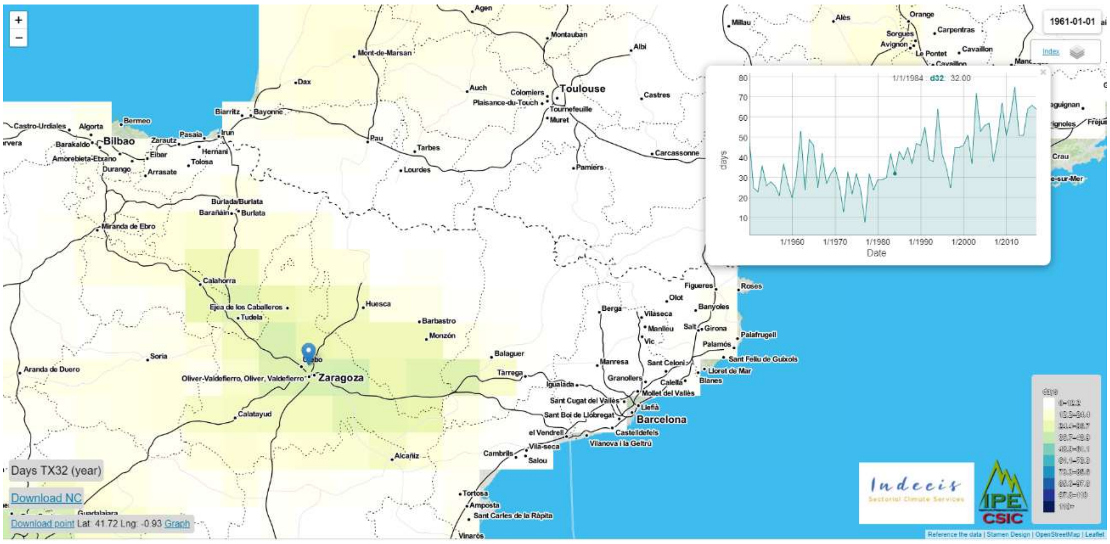

Figure 5: A representative example showing the temporal variability of a selected index (D32: annual temperature sums for days with mean temperature above 32ºC) for a specific grid point.

2.8 Code availability

The code used to calculate the indices is available via: [https://cran.r-project.org/web/packages/ClimInd/index.html.](https://cran.r-project.org/web/packages/ClimInd/index.html) The R scripts necessary to calculate the different indices from the ECA&D and ERA5 gridded datasets in a 3-D array format are provided.

2.9 References

1. Sergio, F., Blas, J. & Hiraldo, F. Animal responses to natural disturbance and climate extremes: a review. *Glob. Planet. Change* **161**, 28–40 (2018).

2. Eyshi Rezaei, E., Webber, H., Gaiser, T., Naab, J. & Ewert, F. Heat stress in cereals: Mechanisms and modelling. *Eur. J. Agron.* **64**, 98–113 (2015).

3. Bachmair, S., Tanguy, M., Hannaford, J. & Stahl, K. How well do meteorological indicators represent agricultural and forest drought across Europe? *Environ. Res. Lett.* **13**, (2018).

4. Olesen, J. E. *et al.* Impacts and adaptation of European crop production systems to climate change. *Eur. J. Agron.* **34**, 96–112 (2011).

5. Wolf, S. *et al.* Contrasting response of grassland versus forest carbon and water fluxes to spring drought in Switzerland. *Environ. Res. Lett.* **8**, (2013).

6. Van Dijk, A. I. J. M. *et al.* The Millennium Drought in southeast Australia (2001-2009): Natural and human causes and implications for water resources, ecosystems, economy, and society. *Water Resour. Res.* **49**, 1040–1057 (2013).

7. Crockett, J. L. & Leroy Westerling, A. Greater temperature and precipitation extremes intensify Western U.S. droughts, wildfire severity, and sierra Nevada tree mortality. *J. Clim.* **31**, 341–354 (2018).

8. Porter, J. R. & Semenov, M. A. Crop responses to climatic variation. *Philos. Trans. R. Soc. B Biol. Sci.* **360**, 2021–2035 (2005).

9. Prugh, L. R. *et al.* Ecological winners and losers of extreme drought in California. *Nat. Clim. Chang.* **8**, 819–824 (2018).

10. Vicente-Serrano, S. M. *et al.* Response of vegetation to drought time-scales across global land biomes. *Proc. Natl. Acad. Sci. U. S. A.* **110**, 52–7 (2013).

11. Ruffault, J., Curt, T., Martin-Stpaul, N. K., Moron, V. & Trigo, R. M. Extreme wildfire events are linked to global-change-type droughts in the northern Mediterranean. *Nat. Hazards Earth Syst. Sci.* **18**, 847–856 (2018).

12. Di Napoli, C., Pappenberger, F. & Cloke, H. L. Assessing heat-related health risk in Europe via the Universal Thermal Climate Index (UTCI). *Int. J. Biometeorol.* **62**, 1155–1165 (2018).

13. Blazejczyk, K., Epstein, Y., Jendritzky, G., Staiger, H. & Tinz, B. Comparison of UTCI to selected thermal indices. *Int. J. Biometeorol.* **56**, 515–535 (2012).

14. Vicente-Serrano, S. M., Beguería, S. & López-Moreno, J. I. A multiscalar drought index sensitive to

global warming: The standardized precipitation evapotranspiration index. *J. Clim.* **23**, 1696–1718 (2010).

15. Matiu, M., Ankerst, D. P. & Menzel, A. Interactions between temperature and drought in global and regional crop yield variability during 1961-2014. *PLoS One* **12**, (2017).

16. Lobell, D. B. *et al.* The shifting influence of drought and heat stress for crops in northeast Australia. *Glob. Chang. Biol.* **21**, 4115–4127 (2015).

17. De Freitas, C. R., Scott, D. & McBoyle, G. A second generation climate index for tourism (CIT): Specification and verification. *Int. J. Biometeorol.* **52**, 399–407 (2008).

18. Scott, D., Gössling, S. & De Freitas, C. R. Preferred climates for tourism: case studies from Canada, New Zealand and Sweden. *Clim. Res.* **38**, 61–73 (2008).

19. Easterling, D. R., Alexander, L. V, Mokssit, A. & Detemmerman, V. CCI/CLIVAR workshop to develop priority climate indices. *Bull. Am. Meteorol. Soc.* **84**, 1403-1407+1329 (2003).

20. Yu, G., Schwartz, Z. & Walsh, J. E. A weather-resolving index for assessing the impact of climate change on tourism related climate resources. *Clim. Change* **95**, 551–573 (2009).

21. Sillmann, J., Kharin, V. V., Zhang, X., Zwiers, F. W. & Bronaugh, D. Climate extremes indices in the CMIP5 multimodel ensemble: Part 1. Model evaluation in the present climate. *J. Geophys. Res. Atmos.* **118**, 1716–1733 (2013).

22. Zhou, B., Wen, Q. H., Xu, Y., Song, L. & Zhang, X. Projected changes in temperature and precipitation extremes in China by the CMIP5 multimodel ensembles. *J. Clim.* **27**, 6591–6611 (2014).

23. Dosio, A. Projections of climate change indices of temperature and precipitation from an ensemble of bias-adjusted high-resolution EURO-CORDEX regional climate models. *J. Geophys. Res. Atmos.* **121**, 5488–5511 (2016).

24. Campozano, L. *et al.* Evaluating extreme climate indices from CMIP3&5 global climate models and reanalysis data sets: a case study for present climate in the Andes of Ecuador. *Int. J. Climatol.* **37**, 363–379 (2017).

25. Klein Tank, A. M. G., Zwiers, F. & Zhang, X. *Guidelines on Analysis of extremes in a changing climate in support of informed decisions for adaptation, WMO/TD-1500, Climate Data and Monitoring WCDMP-No. 72*. (2009).

26. Bezerra, B. G., Silva, L. L., e Silva, C. M. & de Carvalho, G. G. Changes of precipitation extremes indices in São Francisco River Basin, Brazil from 1947 to 2012. *Theor. Appl. Climatol.* **135**, 565–576 (2019).

27. YIN, H. & SUN, Y. Characteristics of extreme temperature and precipitation in China in 2017 based on ETCCDI indices. *Adv. Clim. Chang. Res.* **9**, 218–226 (2018).

28. Wang, H., Pan, Y., Chen, Y. & Ye, Z. Linear trend and abrupt changes of climate indices in the arid region of northwestern China. *Atmos. Res.* **196**, 108–118 (2017).

29. Abatan, A. A., Abiodun, B. J., Gutowski, W. J. & Rasaq-Balogun, S. O. Trends and variability in absolute indices of temperature extremes over Nigeria: linkage with NAO. *Int. J. Climatol.* **38**, 593–612 (2018).

30. Touré Halimatou, A., Kalifa, T. & Kyei-Baffour, N. Assessment of changing trends of daily precipitation and temperature extremes in Bamako and Ségou in Mali from 1961- 2014. *Weather Clim. Extrem.* **18**, 8–16 (2017).

31. Mathbout, S. *et al.* Observed Changes in Daily Precipitation Extremes at Annual Timescale Over the Eastern Mediterranean During 1961–2012. *Pure Appl. Geophys.* **175**, 3875–3890 (2018).

32. Turco, M., Zollo, A. L., Ronchi, C., De Luigi, C. & Mercogliano, P. Assessing gridded observations for daily precipitation extremes in the Alps with a focus on northwest Italy. *Nat. Hazards Earth Syst. Sci.* **13**, 1457–1468 (2013).

33. Supari, Tangang, F., Juneng, L. & Aldrian, E. Observed changes in extreme temperature and precipitation over Indonesia. *Int. J. Climatol.* **37**, 1979–1997 (2017).

34. Terando, A., Easterling, W. E., Keller, K. & Easterling, D. R. Observed and modeled twentieth-century spatial and temporal patterns of selected agro-climate indices in North America. *J. Clim.* **25**, 473–490 (2012).

35. Beharry, S. L., Clarke, R. M. & Kumarsingh, K. Variations in extreme temperature and precipitation for a Caribbean island: Trinidad. *Theor. Appl. Climatol.* **122**, 783–797 (2015).

36. Sajjad, H. & Ghaffar, A. Observed, simulated and projected extreme climate indices over Pakistan in changing climate. *Theor. Appl. Climatol.* (2018). doi:10.1007/s00704-018-2573-7

37. Aerenson, T., Tebaldi, C., Sanderson, B. & Lamarque, J.-F. Changes in a suite of indicators of extreme temperature and precipitation under 1.5 and 2 degrees warming. *Environ. Res. Lett.* **13**, 035009 (2018).

38. Dong, S. *et al.* Observed changes in temperature extremes over Asia and their attribution. *Clim. Dyn.* **51**, 339–353 (2018).

39. Dietzsch, F. *et al.* A global ETCCDI-based precipitation climatology from satellite and rain gauge measurements. *Climate* **5**, (2017).

40. Donat, M. G. *et al.* Global Land-Based Datasets for Monitoring Climatic Extremes. *Bull. Am. Meteorol. Soc.* **94**, 997–1006 (2013).

41. Lorenz, R. *et al.* Representation of climate extreme indices in the ACCESS1.3b coupled atmosphere-land surface model. *Geosci. Model Dev.* **7**, 545–567 (2014).

42. Street, R. B. Towards a leading role on climate services in Europe: A research and innovation roadmap. *Clim. Serv.* **1**, 2–5 (2016).

43. Cornes, R. C., van der Schrier, G., van den Besselaar, E. J. M. & Jones, P. D. An Ensemble Version of the E-OBS Temperature and Precipitation Data Sets. *J. Geophys. Res. Atmos.* **123**, 9391–9409 (2018).

44. Squintu, A. A., van der Schrier, G., Brugnara, Y. & Klein Tank, A. Homogenization of daily temperature series in the European Climate Assessment & Dataset. *Int. J. Climatol.* **39**, 1243–1261 (2019).

45. (C3S), C. C. C. S. ERA5: Fifth generation of ECMWF atmospheric reanalyses of the global climate . Copernicus Climate Change Service Climate Data Store (CDS). (2017).

2.10 Acknowledgements

This work was supported by the research projects PCIN-2015-220, CGL2017-82216-R and CGL2017-83866-C3-1-R financed by the Spanish Commission of Science and Technology and FEDER; CROSSDRO project financed by the AXIS (Assessment of Cross(X) - sectorial climate Impacts and pathways for Sustainable transformation), JPI-Climate co-funded call of the European Commission and INDECIS which is part of ERA4CS, an ERA-NET initiated by JPI Climate, and funded by FORMAS (SE), DLR (DE), BMWFW (AT), IFD (DK), MINECO (ES), ANR (FR) with co-funding by the European Union (Grant 690462). Dhais Peña-Angulo is supported by a "Juan de la Cierva" postdoctoral contract (FJCI-2017-33652 Spanish Ministry of Economy and Competitiveness, MEC).

2.11 Author contribution

Experimental design: Sergio M. Vicente-Serrano, Enric Aguilar, Fernando Domínguez-Castro. Database design: Fernando Domínguez-Castro, Fergus Reig. Data extraction and manipulation: Fergus Reig, Gerard Van der Schrier, Dhais Peña-Angulo. Data visualisation: Fergus Reig. Manuscript writing: Fernando Domínguez-Castro, Sergio M. Vicente-Serrano, Enric Aguilar, Gerard Van der Schrier, Ahmed M. El Kenawy, Iván Noguera, Jesús Revuelto.

“ECTACI: European Climatology and Trend Atlas of Climate Indices (1979-2017)”

3.1 Abstract

A fundamental key to understanding climate change and its implications is the availability of databases with wide spatial coverage, over a long period of time, with constant updates and high spatial resolution. This study describes a newly gridded dataset and its map viewer “European Climatology and Trend Atlas of Climate Indices” (ECTACI), which contains four statistical parameters (climatology, coefficient of variation, slope and significant trend) from 125 standard climate indices for the whole Europe at 0.25º grid intervals from 1979-2017 at various temporal scales (monthly, seasonal and annual). In addition, this study shows, for the first time, the general trends of a wide variety of updated standard climate indices at seasonal and annual scale for the whole of Europe, which could be a useful tool for climate analysis and its impact on different sectors and socioeconomic activities. The dataset and ECTACI map viewer is available for free (http://ECTACI.csic.es/).

3.2 Introduction

Climate has a strong impact on different sectors of society, such as tourism (Amelung and Viner, 2006; Nicholls and Amelung, 2008; Perch-Nielsen et al., 2010), human health (Huang et al., 2011; IPCC 2012; Woodward et al., 2014; Cheng et al., 2015), agriculture (Koufos et al., 2013; Fischer et al., 2005; Moral et al., 2017; Piticar et al., 2018) and ecology (Easterling et al., 2000), among others. Furthermore, economic sectors largely dependent on weather conditions (agriculture, water resources, fisheries, tourism, etc.) are increasingly conditioned by the impacts from climate change (Hoegh-Guldberg et al., 2018). Extreme weather events cause economic loss, as well as to human lives, which together with a society that has become more vulnerable, point to the urgent need to increase our knowledge on climate change (Easterling et al., 2000) and for climate information.

Researchers, policy makers, and the general public are demanding climate services that are more readily applicable to specific areas of society. However, some sectors such as tourism, energy, agriculture, etc., demand tailored information that is not usually directly available. For example, some sectors are affected by the combination of meteorological variables e.g. the combination of temperature, relative humidity and solar radiation is important for the human comfort index, which is used in public health monitoring (Di Nappoli et al., 2018; Goldie et al., 2019). However, other sectors need information on mean values in a specific period of the year, e.g. agriculture during the growing season. To meet these demands, a huge amount of specific climate indices have been created from raw climate variables (Easterling et al., 2003; Yu et al., 2009).

Climate indices are important indicators of the state and changes in the climate system (Williams and Eggieston, 2017). Each climate index is based on certain parameters and describes statistical characteristics defining a time series of climate variables, such as its mean, extreme or trend. Over the past decades, several studies have analyzed changes in climate indices in various regions and periods. WorldClim (Hijmans et al., 2005) global space coverage is a set of global climate layers containing average monthly gridded climate data for the period 1970-2000 at different spatial resolutions. This dataset includes the minimum, mean, and maximum temperature, precipitation, and derived bioclimatic indices. Alexander et al., (2006) also used global space coverage to make a study on the changes in daily climate extremes of temperature and precipitation for different periods. In Europe, studies have analyzed changes in climate indices. The joint CCl/CLIVAR/JCOMM Expert Team (ET) on Climate Change Detection and Indices (ETCCDI) developed of a suite of climate change indices primarily focusing on extremes (Frich et al., 2002, Alexander et al., 2006, Klein Tank et al., 2003, Klein Tank et al., 2009), and developed software to calculate climate indices. The core set of 27 extreme indices developed by ETCCDI is commonly used in climate studies worldwide, e.g. China (Hong and Yin, 2018), India (Panda et al., 2016) and Europe (Van den Besselaar et al., 2013).

On the other hand, the EMULATE project (European and North Atlantic daily to MULtidecadal climate variability) carried out systematic mapping of the trend observed in 64 temperature and precipitation indices based on daily instrumental records for the period 1901-2000 (Moberg et al., 2006); however, access is limited (Chen et al., 2015). Additionally, Klein Tank and Können (2003) examined trends in the six indices for daily temperature and seven indices for precipitation extremes for the period 1946-1999 from more than 100 stations in Europe. This study found symmetric warming of the cold and warm tails on the distribution of daily minimum and maximum temperatures for several periods: from 1946-1975 slight cooling occurred, and from 1976-1999 warming became more apparent and the number of wet days increased. The same study also indicated the need to carry out research using a higher density of weather stations. Several studies on the trend of climate indices have also been carried out on a national level, e.g. China (Yin, 2018), the western Indian Ocean (Vincent et al., 2011), USA (Heim, 2015), southwestern Spain (Moral et al., 2016), Turkey (Toros, 2012) and Cyprus (Katsanos et al., 2018), among others. General conclusions and questions emerge from these findings: (i) the low density of weather stations and especially their irregular spatial distribution has not prevented a comprehensive picture of the climate indices from being obtained; (ii) most studies focus on temperature and precipitation indices, with very few involving other types of climate indices; (iii) most studies focus on climatic indices that evaluate extreme events.

This paper aims to provide a comprehensive analysis of the climatology and recent temporal evolution of seasonal and annual values from 117 climate indices covering the whole of Europe in the period 1979-2017. Following an exhaustive literature review, these were deemed the most important ones for the priority sectors of the Global Framework for Climate services i.e. agriculture, disaster risk reduction, energy, health, water and tourism. This was the first time a wide variety of climate indices for the whole of Europe had been used, and estimated with updated data and high spatial resolution. The main objectives were: i) to generate a spatial climatology from the indices in order to understand climate characteristics beyond the climatology of average values, and ii) to find changes in these indices over the last four decades at seasonal and annual scales. Furthermore, this study presents a new gridded dataset and map viewer (ECTACI: European Climatology and Trend Atlas of Climate Indices) showing monthly, seasonal and annual climatology, coefficient of variation and trend from 125 climate indices in Europe (1979-2017).

3.3 Data and Methods

Climate indices

This study uses the "ClimInd" package within the R platform (https://cran.r-project.org/web/packages/ClimInd/index.html) to compute 125 climate indices at monthly, seasonal and annual temporal frequency for Europe (125 at monthly scale and 117 at seasonal and annual scale). The specific definition for each index can be seen in Figure 6 and details of the climate index dataset can be found in Domínguez-Castro et al. (2020). The 125 climate indices were selected from a review of the literature (Frich et al., 2002; Klein Tank et al., 2003; Alexander et al., 2006; among others) and their impact on the high-priority sectors (agriculture, disaster risk reduction, energy, health, water, and tourism), and grouped into eight categories: temperature (42), precipitation (21), bioclimatic (21), aridity/continentality (10), cloud/radiation (5), wind (6), snow (12) and drought (8).

Temperature	
CFD	Maximum consecutive frost days
CSD	Maximum number of consecutive summer days
CSDI	Cold spell duration
D32	Days with maximum temperature > 32ºC
DD17	Difference days above/below with TXx 17ºC
DTR	Diurnal temperature range
ETR	Extreme temperature range
FD	Frost days
GD4	Growing degree days
GSL	Growing season length
GTG	Mean average temperature
GTN	Mean minimum temperature
GTX	Mean maximum temperature
HD17	Heating degree days
ID	Ice days
NTG	Minimum mean temperature
OGS6	Onset of growing season 6 days
OGS10	Onset of growing season 10 days
PTG	Sums positive
STN10	Sums minimum temperature < 10ºC
STN15	Sums minimum temperature < 15ºC
STX32	Sums maximum temperature > 32ºC
SU	Summer days
Ta_o	Growing season (Apr-Oct)
Tm_s	Growing season(May-Sep)
TN10p	Cold nights
TN90p	Warm nights
TNn	Minimum minimum temperature
TXn	Minimum maximum temperature
TR	Tropical nights
TX10p	Cold days
TX90p	Warm days
TNx	Maximum minimum temperature
TXx	Maximum maximum temperature
VCD	Very cold days
vDTR	Mean daily difference DTR
VWD	Very warm days
WKI	Winkler index
WS	Winter Severity
WSDI	Warm spell duration
XTG	Maximum mean temperature
ZCD	Zero crossing days

Precipitation	
CDD	Longest dry period
CWD	Longest wet period
D50mm	Heavy precipitation days
D95p	Very wet days
DD	Dry days
DR1mm	Wet days 1mm
DR3mm	Wet days 3mm
EP	Effective precipitation
GSR	Growing season precipitation (Apr-Oct)
MFI	Modified Fournier Index
NGSR	Non-growing season precipitation (Oct-Apr)
PCI	Precipitation Concentration Index
PRCPTOT	Total precipitation wet days
R10mm	Days precipitation ≥ 10mm
R20mm	Days precipitation ≥ 20mm
R95tot	Precipitation fraction very wet days
R99tot	Precipitation fraction extremely wet days
RT	Total precipitation
RX1day	Maximun precipitation
Rx5day	Maximum 5 days precipitation
SDII	Simple daily intensity index

Wind	
BI	Budyko Index
CMD	Climatic moisture deficit
EAI	Emberger aridity index
ETo	Reference evapotranspiration
JCI	Johansson Continentality Index
KOI	Kerner Oceanity Index
MAI	De Martonne aridity index
MOI	Marsz Oceanity Index
PiCI	Pinna Combinative index
UAI	UNEP aridity index

Aridity/Continentality	
DFx21	Days wind gusts above 21 m/s
FG	Mean of daily mean wind strength
FG6Bft	Days daily averaged wind above 10.8m/s
fgcalm	Calm days
FXx	Daily maximum wind gust

Cloud/Radiation	
ACI	Atmospheric Clarity Index
CC	Mean daily cloud cover
FOD	Foggy days
SND	Sunny days
SSD	Sum of sunshine duration
SSp	Sunshine duration fraction

Bioclimatic	
AT	Apparent temperature
BIO4	Temperature seasonality
BIO5	Maximum temperature warmest month
BIO6	Maximum temperature coldest month
BIO7	Difference warmest/coldest month
BIO8	Mean temperature of wettest quarter
BIO9	Mean temperature of driest quarter
BIO10	Mean temperature of warmest quarter
BIO11	Mean temperature of coldest quarter
BIO13	Precipitation of wettest month
BIO14	Precipitation of driest month
BIO15	Coefficient of variation precipitation
BIO16	Precipitation of wettest quarter
BIO17	Precipitation of driest quarter
BIO18	Precipitation of warmest quarter
BIO19	Precipitation of coldest quarter
BIO20	Mean radiation
HI	Heat index
MI	Mould index
UTCI	Universal thermal climate index
WCI	Wind chill index
SDII	Simple daily intensity index

Snow	
ASD	Average snow depth
FPSC	Date of first permanent snow cover
FSC	Date of first snow cover
FSD	Frequency of snow days
HSD	Heavy snowy days
LPSC	Date of last permanent snow cover
MS	Maximum snow depth
MSD	Mild snowy days
SCD	Amount of snow covered days
SD0_10	Snow days depth 1-10
SD10_20	Snow days depth 10-20
SS	Snowfall sum

Drought	
SPI1	Standardized precipitation index 1
SPI3	Standardized precipitation index 3
SPI6	Standardized precipitation index 6
SPI12	Standardized precipitation index 12
SPEI1	Standardised Precipitation-Evapotranspiration Index 1
SPEI3	Standardised Precipitation-Evapotranspiration Index 3
SPEI6	Standardised Precipitation-Evapotranspiration Index 6
SPEI12	Standardised Precipitation-Evapotranspiration Index 12

Figure 6. Climate indices (abbreviation and definition) used in this study.

A gridded database of the 125 climate indices was generated from the European Climate Assessment and Dataset (ECA&D) E-OBS gridded dataset v17.0 (Cornes et al., 2018) and the ERA5 reanalysis database (Copernicus Climate Change Service, 2017). The ECA&D dataset contains quality-controlled meteorological records, sourced from the European National Meteorological Services, and the E-OBS is the gridded dataset based on the information from these stations. The ERA5 is the latest generation of the reanalysis dataset developed by the European Center for Medium-Range Weather Forecasts (EWMF). We used ERA5 data to obtain the climate variables not found in the observational dataset. In spite of the different characteristics of both databases, we unified the criteria of the two to work with the same spatial cover (0.25º, 12280 time series), temporal (monthly, seasonal and annual), and period (1979-2017) throughout Europe. In some cases, the climate index was calculated only on annual scale. Indices requiring a base period for their calculation took the entire period as a reference (i.e. TX10p, TX10p, CDD, VCD, VWD, TX90p, TN90p, WSDI, R95tot, R99tot, D95p).

Statistical analysis

The study obtained four statistics for each climatic index and for 12280 series covering Europe at monthly, seasonal and annual scales for the whole period (1979-2017): (1) mean climatology, (2) coefficient of variation in order to find the interannual variability, (3) slope of the linear model in order to find the magnitude of change, and (4) trend significance by means of the Mann Kendall test. The linear trend was estimated by the Ordinary Least Squares method; which is widely used in climate studies (Kiktev et al., 2003; Moberg and Jones, 2005; Moberg et al., 2006). The trend significance at levels of $p < 0.05$ and $p < 0.01$ was evaluated with the Mann-Kendall test taking into account serial correlation (Kiktev et al., 2003, Alexander et al., 2006). Positive/negative signals are expressed by colors (red/blue) and the significance in the Mann–Kendall test is shown by three color variations, not significant, significant at p level < 0.05 and significant at p level < 0.01. The ECTACI dataset and map viewer contain the spatial distribution of the four statistics: climatology, coefficient of variation, slope and significant trend. The statistical analyses applied to the 125 climate indices were checked for consistency in their spatial distribution from map viewer.

For the first time, many of the climate indices were included in the same spatial and study period at different temporal scales. Consult Figure 6 when analyzing the results and discussion section of this study, which includes abbreviations, names and temporal scales of the climate indices. In the results section, the climatology and trend of the 117 indices at seasonal and annual scales are shown by percentage of land with positive and negative trends in all indices and spatial distribution of statistics of those selected which are a good example of the rest of the indices of each category (Temperature: FD and GTG, Precipitation: RT, Aridity/Continentality: CDM, Cloud/Radiation: CC and SSp, Wind: FXx, and Snow: FSD, see Figure 6 for abbreviations used). The selected climate indices belong to each category in the study and represent an example of the behavior of the other indices according to their category. Furthermore, it presents a new gridded dataset and map viewer (ECTACI) showing the monthly, seasonal and annual climatology, coefficient of variation and trend of the 125 climate indices in Europe (1979-2017).

All statistical procedures, maps and plots used the R statistical programming language (R Core Team and R Development Team Core, 2017), packages “ClimInd” climatic indices; ncdf4 for netcdf format; maptools, maps, rgeos, raster and rgdal for spatial data manipulation; and ggplot2 for mapping and plotting.

3.4 Results

Annual and seasonal trend of climate indices throughout Europe

Climatology of climate indices throughout Europe

The spatial climatology of selected climate indices across the Europe is shown in Figure 7 through reporting statistical parameters (mean and coefficient of variation) for each grid cell of the ECTACI dataset at annual scales from 1979-2017. Maximum values from FD index climatology (Figure 7a) were recorded over northern Europe (Norway, Sweden, Finland, Iceland) and mountain areas (Alps, Carpathians, Pyrenees); while minimum values were recorded in southern Europe, especially in the Mediterranean area. The climatology of GTG (Figure 7b) and SSP (Figure 7f) indices have a strong latitudinal component, with maximum values in the south and minimum values in the north of the study area. The opposite is true of the CC index (Figure 7e), which has maximum values in the north and minimum values in the south. The maximum climatology from the RT index (Figure 7c) was measured in the northwest of the Scandinavian Peninsula, British Isles, Iberian Peninsula and the Alps. CMD index maximum values (Figure 7d) were recorded in the south of the Iberian Peninsula. On the other hand, the FXx index (Figure 7g) showed a west-east spatial pattern, with maximum values in the west and minimum values in the east. The maximum FSD index climatology (Figure 7h) was measured in the Scandinavian Peninsula, Iceland and mountain areas, while minimum values were found in southwest Europe, especially in the Iberian Peninsula. Lastly, the spatial variability of the selected climate indices is illustrated by the coefficient of variation (Figure 7).

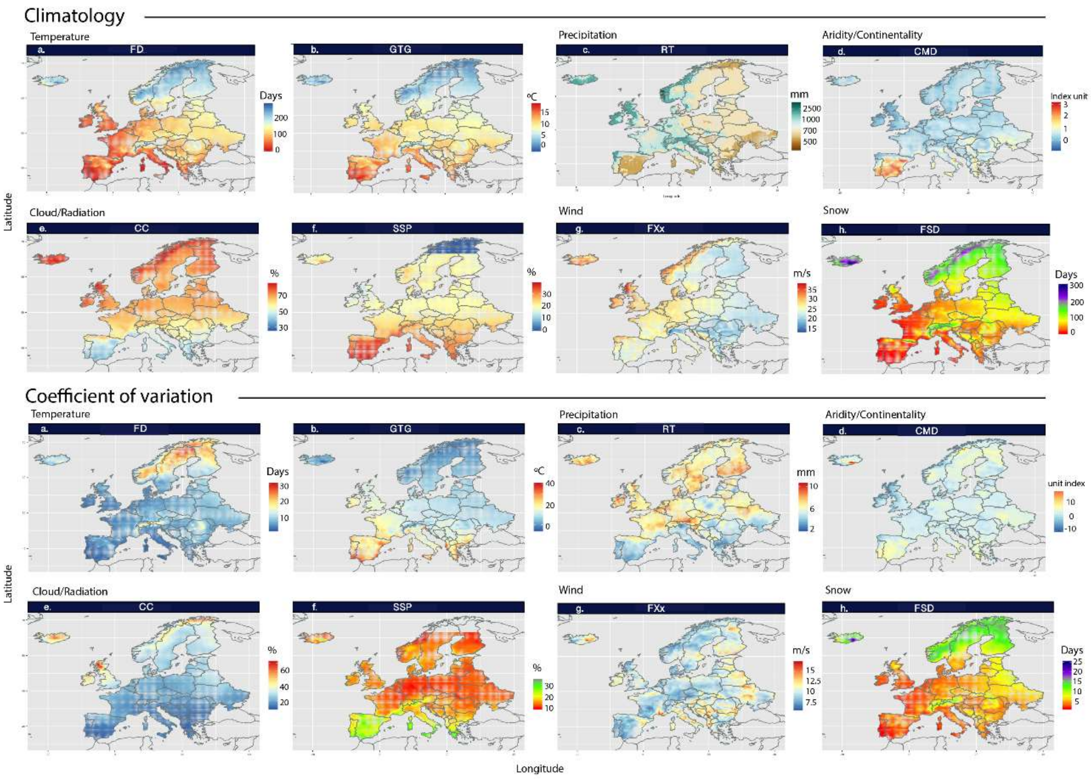

Figure **7. Annual spatial distribution of the climatology and variability of eight climate indices for Europe in the period 1979-2017. Each index belongs to one of six categories, temperature: a.) FD and b.) GTG, precipitation: c.) RT, aridity/continentality: d.) CMD, cloud/radiation: e.) CC and f.) SSP, wind: g.) FXx, snow: h.) FSD.**

Spatio-temporal annual trends of climate indices throughout Europe

In general, the spatial variability of the trend in annual climate indices is important. Spatial behaviour can be summarized into three categories: i) climate indices with a high percentage of land (more than 75%) with a positive trend, ii) climate indices with a high percentage of land (more than 75%) with a negative trend and iii) climate indices that do not show a clear positive or negative trend (more than 25% and less than 75% of the land). The trend in annual climate indices can be observed in Figure 8, which depicts the percentage of land with positive or negative trends, significant (p level <0.05) or not significant (p level >0.05) of the 117 climate indices at annual scale in Europe. Following the order of the previously defined categories, the climate indices showing more than 75% of land with a positive trend are: for temperature: CSD, DD17, GD4, GSL, GTG, GTN, GTX, NTG, TNn, TXn, PTG, SU, Ta_o, Tm_s, TN90P, TX90P, VWD, WKI, WS, WSDI, XTG, TNx, TXx; for aridity/continentality: ETo; for cloud/radiation: ACI, SND, SSD, SSp. On the other hand, the climate indices with a negative trend in more than 75% of land are: for temperature: CFD, CSDI, FD, HD17, ID, OGS10, OGS6, STN10, STN15, TN10P, TX10P, VCD; for aridity/continentality: KOI; for cloud/radiation: CC, FOD; for snow: ASD, FSD, LPSC, MS, SCD, SD0_10, SS. Finally, climate indices that do not show a clear positive or negative trend (more than 25% and less than 75% of land) are for temperature: DTR, ETR, vDTR, ZCD; for wind: DFX21, FG, FG6BFT, fgcalm, FXx; and for snow: FPSC, FSC. The major part of the precipitation and aridity/continentality indices are characterized by a very diverse trend throughout space. The snow indices HSD and SD10-20 do not have a clear spatial representation of the trend (less than 25% of land with positive and negative trends).

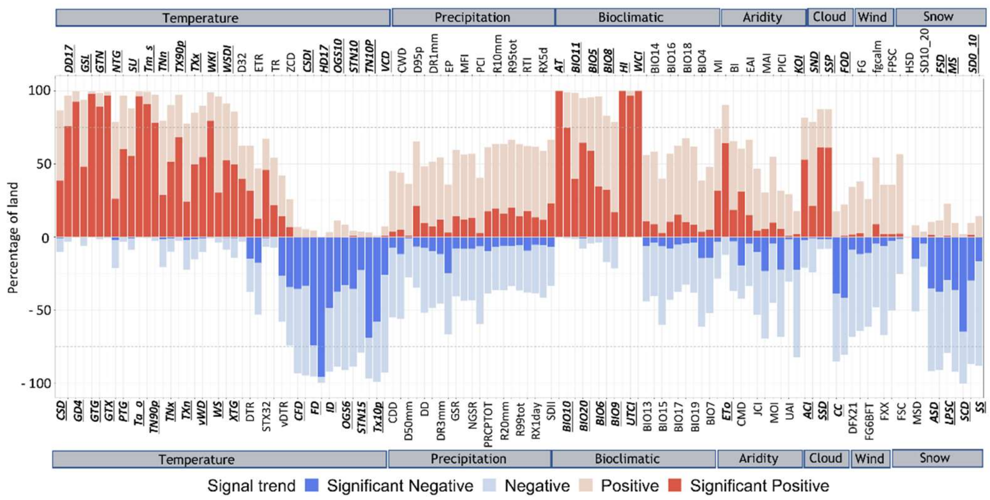

Figure 8**. Percentage of land with a positive or negative trend, significant (p level < 0.05) or non-significant (p level > 0.05) of the 117 climate indices at annual scale in Europe. The bold, underlined and italic indices indicate more than 75% of land with positive or negative trend.**

From the previous results, general patterns in the annual trend of categories in the study could be extracted, summarized in Figure 9. The temperature indices were divided between those with a negative trend and indicate cold days and nights, such as the FD index (Figure 9a), while other indices showed a positive trend and indicate warm days and nights, such as the GTG index (Figure 9b). Most precipitation indices had a large spatial variety in their trend, e.g. RRT (Figure 9c). The indices included in the bioclimatic category were divided between the ones with trends very similar to those of temperatures and those that are similar to precipitation. The aridity/continentality indices showed spatial differences in their trends, e.g. CMD (Figure 9d). On the contrary, indices included in the cloud/radiation category differed between those reflecting the characteristics of the cloudiness with a negative trend, e.g. CC (Figure 9e), and those reflecting the characteristics of the radiation with a positive trend, e.g. SSP (Figure 9f). The indices in the wind category did not generally show a clear trend, but were sometimes negative, e.g. FXx (Figure 9g). Finally, the indices included in the snow category showed a negative trend, with the exception of the very coldest areas in Europe, e.g. FSD (Figure 9h).

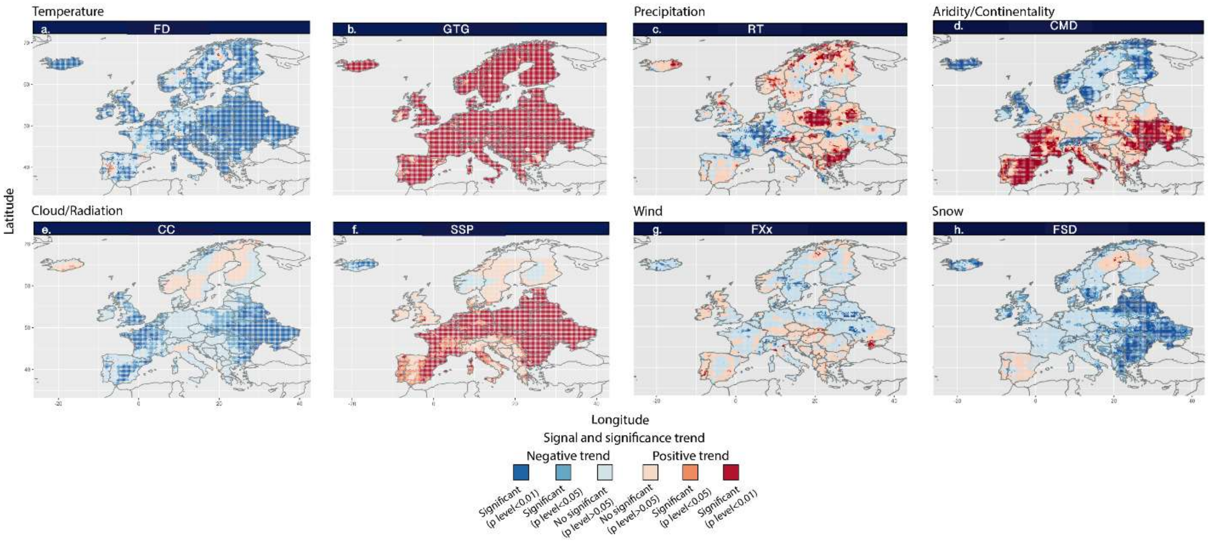

Figure 9. **Spatial distribution of the trend of eight climate indices. Each index belongs to one of six categories, temperature: a.) FD and b.) GTG, precipitation: c.) RT, aridity/continentality: d.) CMD, cloud/radiation: e.) CC and f.) SSP, wind: g.) FXx, snow: h.) FSD at the annual scale for Europe (1979-2017). The positive/negative signal is shown in color (red/blue), and the significance from the Mann–Kendall test is given in three colors variations, non-significant, significant at p level < 0.05 and significant at p level < 0.01.**

In the trend analysis, in addition to obtaining the sign and significance of the trend, we analyzed the magnitude of change. Figure 10 shows the spatial distribution of the magnitude of trend in each selected climate index. The major decrease in the FD index (Figure 10a) was located in the inland areas of Europe, while a strong increase in the GTG index (Figure 10b) occurred in the same area. On the other hand, a clear decrease in the RT index (Figure 10c) was observed in France and its surroundings. The CMD index (Figure 10d) showed spatial differences in their trends, with the largest increase in the south, and the largest decrease in the north of the study area. The CC (Figure 10e) and SSP (Figure 10f) indices had an opposite trend, with the largest decrease in trend found in the CC index and the largest increase in trend in the SSp index corresponding to inland areas of Europe. The FXx index (Figure 10g) showed great spatial variability, with a high increase in some areas, such as the Scandinavian Peninsula, and other areas with a decrease, e.g. Ireland. Finally, the maximum decrease in the FSD index (Figure 10h) was observed in the Scandinavian Peninsula, Iceland, British Islands, and the inland areas of Europe.

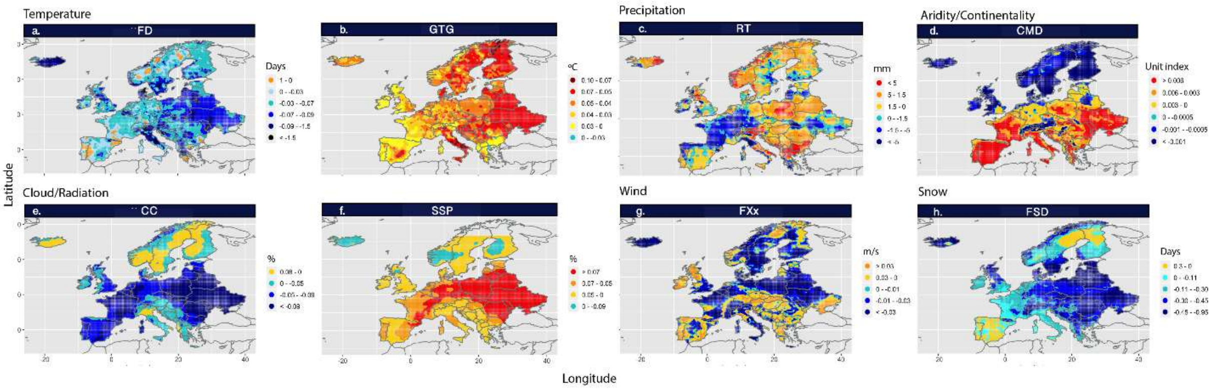

Figure 10**. Spatial distribution of the magnitude of the trend of eight climate indices at annual scale for Europe (1979-2017). Each index belongs to one of six categories, temperature: FD and GTG, precipitation: RT, aridity/continentality: CMD, cloud/radiation: CC and SSP, wind: FXx, snow: FSD.**

Spatio-temporal seasonal trends of climate indices throughout Europe

In addition to the differences observed in the trends of the defined categories, spatial and seasonal differences could also be found. The spatial differences seen in the trends are complex to analyse since there is no continuous pattern, due to several causes, such as orography, areas distant from the sea and latitude, among others. There were different patterns in the seasonal trend of the climate indices selected for the period and study area, which are summarized in Figure 11 and Table S1.

Figure 11 contains the percentage of land with a significant trend in more than 25% of the land in all season. The temperature indices with a significant trend in more than 25% of the land in all seasons, but having a positive signal are GTG, GTN, GTX, TNn and TN90p, while those with negative signal are HD17 and TN10p. On the other hand, the temperature indices with a significant trend in more than 25% of the land in spring, summer and, occasionally, also in autumn with a positive signal are NTG, TXn, TX90p, TNx, XTG and TXx, while a negative signal is found in TX10p. There are some temperature indices with positive and negative trends in different seasons e.g. DTR with a negative trend in winter and a positive trend in spring and summer, and vDTR with a negative trend in autumn and winter, and a positive trend in spring. Lastly, the WSDI index has a positive trend in summer and autumn, and VCD has a negative trend in summer. The temperature indices based on a threshold (e.g., FD, CFD, GD4, DD17, OGS6, OGS10, ID, ZCD) are not included in this section because it is not possible to make a seasonal comparison.

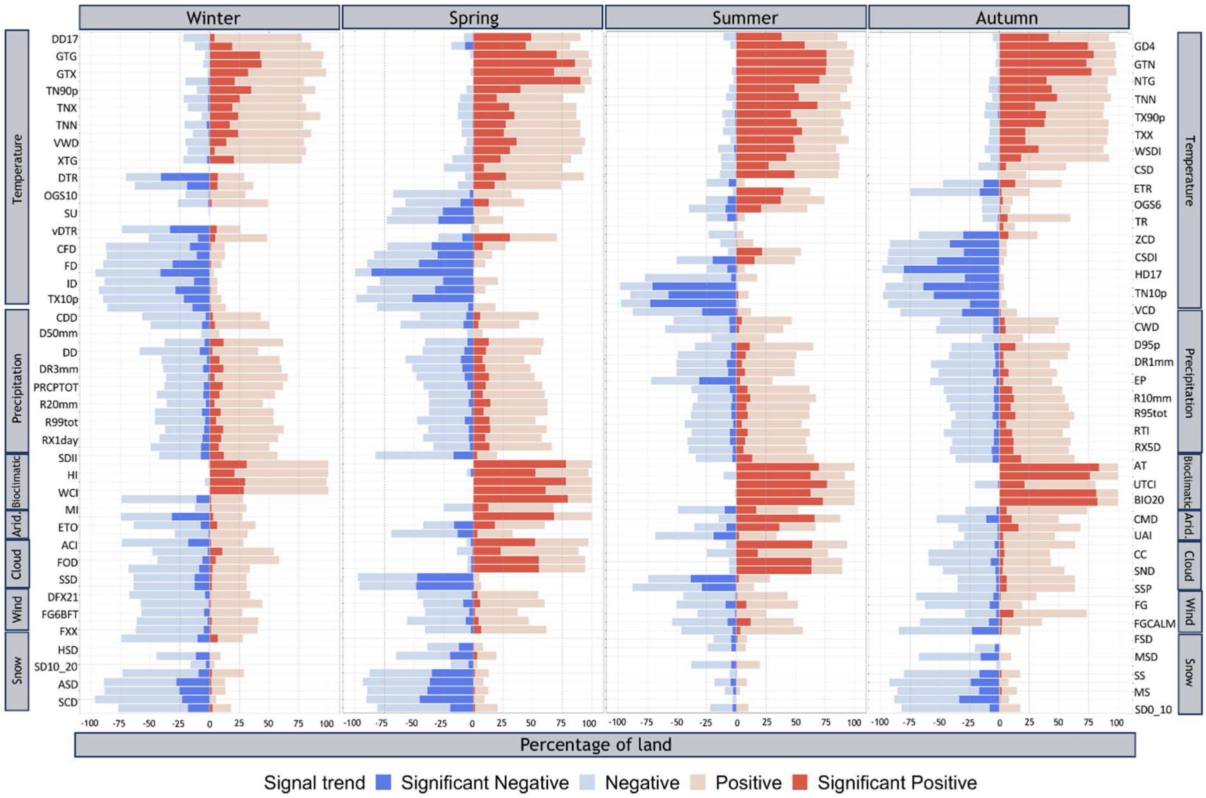

Figure 11**. Percentage of land with a significant (p level < 0.05) positive or negative trend of the 117 climate indices in winter, spring, summer and autumn in Europe.**

For precipitation indices, the trend is only significant in more than 25% of the land in the EP index, with a negative trend in summer. Moreover, the aridity/continentality indices do not have a clear significant trend throughout the study area, only the ETo index has a positive trend in spring and summer, and CMD has a negative trend in winter and positive trend in summer. In all case, the cloud/radiation indices show a clear significant trend in spring and summer with a positive signal in the SSD, SSP and ACI indices, and negative signal in CC and FOD. The wind indices do not show a significant trend. Finally, the snow category has a significant negative trend in winter, spring and autumn in the ASD and MS indices; while this changes to the FSD and SCD indices in spring, and the SCD index in autumn. Most climate indices show that the seasons with the largest changes in their signal trends are summer, followed by spring and autumn; while winter returns the lowest percentage of land affected by changes in trends.

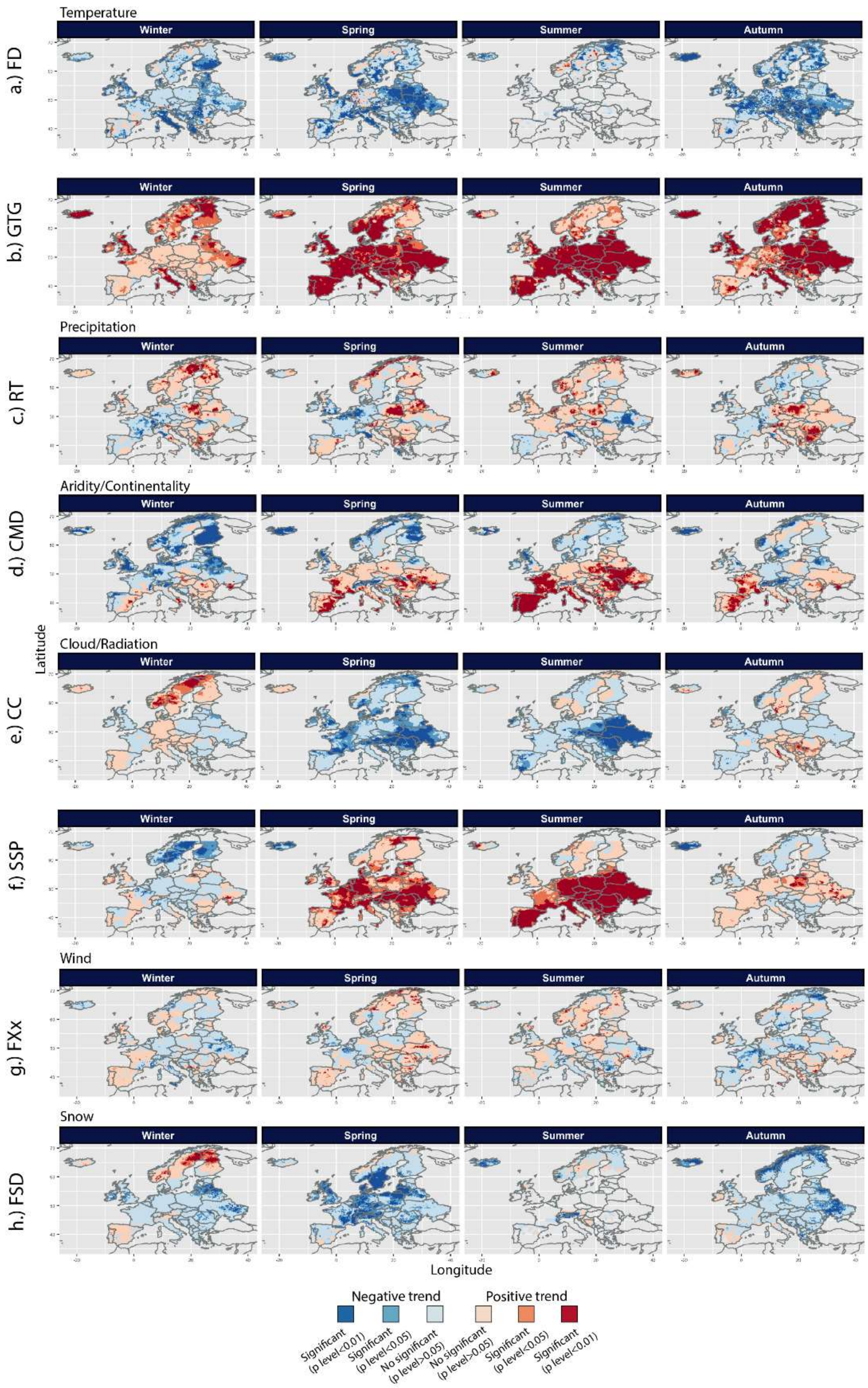

Figure 12**. Spatial distribution of the trend of eight climate indices. Each index belongs to one of six categories, temperature: FD and GTG, precipitation: RT, aridity/continentality: CMD, cloud/radiation:**

CC and SSP, wind: FXx, snow: FSD at seasonal scale (Winter, Spring, Summer, and Autumn) for Europe (1979-2017). The positive/negative signal is shown in color (red/blue), and the significance from the Mann–Kendall test is given in three colors, non-significant, significant at p level < 0.05 and significant at p level < 0.01.

Figure 12 shows the spatial distribution of the seasonal trends of the eight indices selected, ordered by categories. In the temperature category, the FD index shows a significant negative trend in most of the territory in winter, spring and autumn (Figure 12a), while the GTG index has a significant positive trend for the whole of Europe in spring, summer, and autumn (Figure 12b). In precipitation category, RT does not show a clear significant trend (Figure 12c). For aridity/continentality, CMD has two spatial patterns, a significant positive trend in south and a significant negative trend in north of the study area, especially in spring and summer (Figure 12d). Cloud/radiation shows a significant negative trend in the CC index (Figure 12e) and a positive trend in SSP (Figure 12f) in spring and summer across most of the territory. In the wind category, the FXx index does not show a clear significant trend (Figure 12g). Finally, there is a negative trend in the FSD index in winter, spring, and autumn in the snow category (Figure 12h).

Features of the ECTACI dataset and map viewer

The climatology, coefficient of variation, slope and trend significance statistics of 125 climate indices at monthly, seasonal and annual scale for Europe (1979-2017) are included in the ECTACI map viewer. This viewer is structured on different levels (Figure 13): the first level corresponds to the eight categories (temperature, precipitation, bioclimatic, aridity/continentality, cloud/radiation, wind, and snow), the second to the climatic index in each category, the third to the four statistics (climatology, coefficient of variation, slope, and significant trend), and the fourth level to the temporal scale (monthly, seasonal and annual).

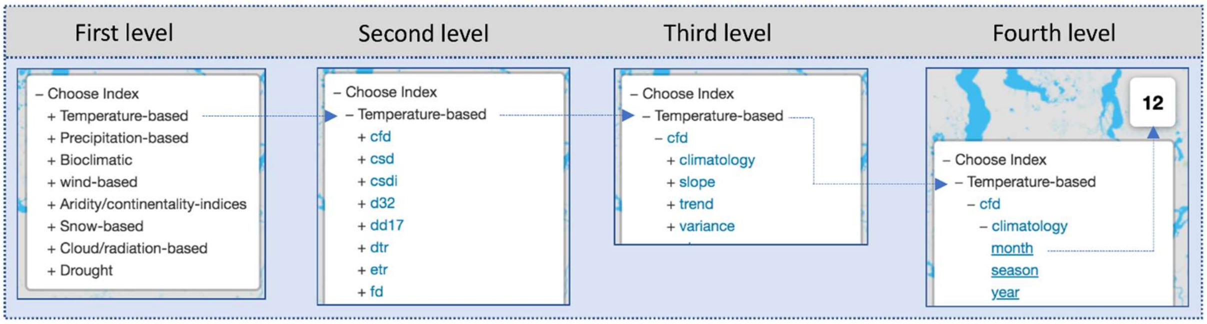

Figure 13**. Structure level of the ECTACI map viewer.**

The monthly scale can be selected from 1 (January) to 12 (December), while the seasonal scale ranges from 1 (winter: DJF) to 4 (autumn: SON). The ECTACI viewer includes basic information on the climate index (ID, name, description, importance and time scale). Furthermore, the viewer can display the exact value of each statistic together with the graphic representation used by the legend (Figure 14). All information available in the ECTACI map viewer can be downloaded in 3-D NetCDF 4 format, available on the website http://ECTACI.csic.es/, maintained by the Spanish National Research Council. Each file download has an array of longitudes (464) x latitudes (201) x time (39 annual scale, 156 seasonal scale, and 468 monthly scale) for the period 1979-2017.

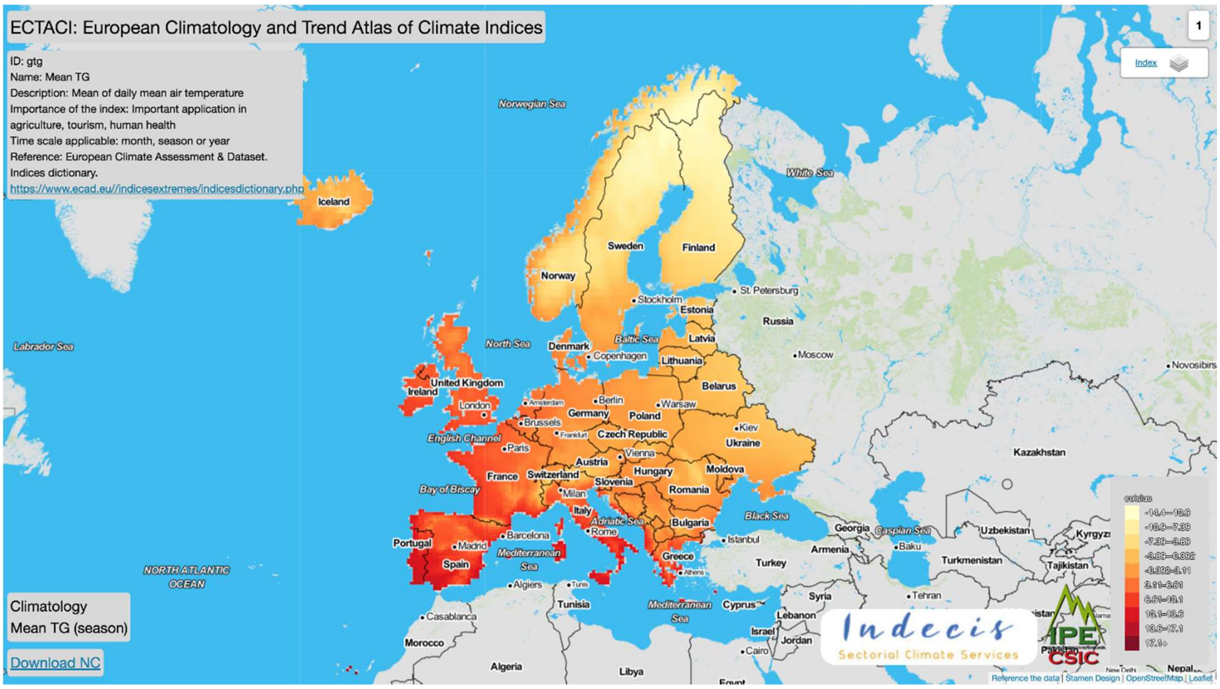

Figure 14. **Web-tool to visualize the statistics (climatology, coefficient of variation and slope and significant trend) of the 125 standard climate index in the ECTACI viewer and download the entire dataset.**

3.5 Discussion

Spatio-temporal annual trends of climate indices throughout Europe

Assessing climate processes and impact is highly complex, since they are difficult to quantify and because of their subjectivity. In this context, the climate indices are useful tools in understanding the variability and impact of the climate on important sectors of society. Climate indices monitor the variations and changes in climate by examining different aspects of the raw variables; therefore, they usually help to inform users of the state of the climate. However, robust climate indices require databases built over the long-term, and characterized by high spatial resolution and extended spatial coverage so that they provide reliable information that is a true reflection of the dimension of climate change and its implications.

In this study, a special effort has been made to unify a large number of climate indices, and analyze their temporal evolution throughout the study area (Figure 12). There are several studies on temperature and precipitation indices which quantify extremes (e.g. TN10p, TX90p), crossing thresholds (e.g. R10mm, R20mm), and the average (e.g. GTG, GTX, GTN) (Frich et al., 2002, Klein and Könner, 2003, Moberg et al., 2006, Alexander et al., 2006, Zhang et al., 2011, IPCC 2012). There are other, less frequent climate indices that have heavy repercussions in certain sectors of society, such as agriculture e.g. GD4, OGS6, PTG, GSR (Winkler et al., 1974, Karl et al., 1999, Martin-Vide 2004, Gabriels 2006, Klein Tank et al., 2009). Bioclimate indices are obtained from the WorldClim dataset (Hijmans et al., 2005, Fick and Hijmans, 2017), which has been used extensively in agricultural, ecological and hydrological assessments (Fick and Hijmans, 2017). There are other, less frequent bioclimate indices, which have importance in tourism and health sectors, like UTCI, MI, HI, WCI, AT (Steadman et al., 1984, Bröde et al., 2012, Osczevski and Bluestein 2005, Di Nappoli et al., 2018).

The aridity/continentality indices are widely used in the ecology and agriculture sectors, due to the importance of plant-available water, e.g. BI, JCI, KOI, PiCI, MAI, MOI (Creed et al., 2014; Baltas 2007). In addition, there are studies indicating that climate change will increase aridity globally as the rising temperatures drive up rates of evapotranspiration (Dai 2011), so different aridity indices are applied, such as CMD, UAI, ETo, and EAI (Wallén, 1967; McGregor, 1988; Chiew et al., 1995; Girvetz and Zganjar, 2014; Huang et al., 2016; Parks et al., 2018). Most studies on cloudiness and radiation use data from surface solar radiation or sunshine indices e.g. SSD, SSP, and CC (Wild 2005; Sanchez-Lorenzo et al., 2008; Stjern et al., 2009; Sanchez-Lorenzo et al., 2015).

In addition, the cloud/radiation indices are used to assess tourism and leisure facilities, e.g. FOD and SND (Blazejczyk, 2006; Rudel et al., 2007). Wind energy is non-polluting cost-effective and renewable, so wind indices, such as DFx21 and FG6Bft, are a valuable source of information (Azad el al., 2010). In addition, wind has substantial impact on society and the environment (human safety, maritime and aviation activities, among others). For this reason, the FG and FXx indices are very useful in recognizing the temporal evolution of mean and maximum wind gust (Azorin-Molina et al., 2016).

On the other hand, the fgcalm index is valuable in studies on pollution in urban areas (Croxford, 1996). Finally, snow indices are widely used to assess the relationship between the winter tourism demand and snow depth, e.g. ASD and MS (Falk, 2010; Pickering, 2011). Fontrodona et al. (2018) indicated a decrease in maximum and mean snow depth over Europe and this has strong implications for the availability of fresh water in spring.

This study has compiled the general trend from the wide variety of climate indices at seasonal and annual scales for Europe (1979-2017). In general, the results obtained are consistent with the review of the literature. The analysis of trends in temperature indices at annual scale showed general warming during the study period 1979-2017, the indices for cold days and night had a negative trend, while the warm days and nights showed a positive trend (Frich et al., 2002; Klein Tank and Können, 2003; Alexander et al., 2006; IPCC 2012). Klein Tank and Können (2003) indicated positive trends in Europe for the indices of wet extremes from 1976-1999. Similarly, Frich et al., (2002) highlighted a significant increase in most heavy precipitation indicators for parts of Europe from 1946-1999. However, Alexander et al., 2006 found that the trend of precipitation indices had poor spatial coherence for the period 1951–2003. In this study, the majority of precipitation indices did not show a general trend for the whole of Europe, but depending on the index, large spatial differences were found. For example, the RT index had a positive trend in the northern and central areas of Europe, but western regions returned a negative trend.

A number of previous studies showed declining rates of near-surface wind speed (termed 'stilling'), which has a significant effect on the climate, such as atmospheric evaporative demand (Vautard et al., 2010; McVicar et al., 2012). In this study, a negative trend predominated in the wind indices, but was not significant in the major part of the study area. On the other hand, this study showed that the indices relating to cloudiness (CC and FOD) had a negative trend, while those for radiation (ACI, SND, SSD, SSp) were positive. Since the 1980s, there has been stabilization and recovery in surface shortwave radiation (termed 'brightening') in many regions of the world (Sanchez-Lorenzo et al., 2015). There are studies explaining the brightening phenomenon due to variations in anthropogenic aerosol emissions and/or cloudiness (Wild, 2009; Sanchez-Lorenzo et al., 2015). Furthermore, Tang et al. (2012) demonstrated that summer temperatures in Europe have undergone a dramatic rise in tandem with decreased cloud cover and increased surface solar radiation. Finally, snow indices returned a negative trend across most of the territory studied. This agreed with the study by Kunkel et al. (2016) that indicated the maximum snow depth decreased in European stations from 1960-2015. In addition, Fontrodona et al. (2018) found decreases in maximum and mean snow depth across Europe, except in the coldest climates, from 1951 onward.

Spatio-temporal seasonal trends of climate indices throughout Europe

The overall results of trend estimation, taking into account the signal and significance trend over most of the territory studied, show clear seasonality according to the climate indices. For temperatures: the daily, maximum and minimum mean temperatures, the number of warm nights and the temperature of the coldest nights increased in all seasons. Conversely, the number of cold nights and the heating degree days, a measure for the energy needed to heat buildings, decreased throughout Europe in all seasons. However, the number of warm nights and the maximum and minimum of the mean and maximum temperatures increased, while the number of cold days decreased in summer and spring, and occasionally in autumn. There are abundant studies on the temperature trends in Europe; however, the comparison between them is complex, since the temporal scale (annual or seasonal), or the spatial resolution vary in the study period. Moberg & Jones (2005) highlight "the warming of winters during 1946 – 99 occurred in both the warm and cold tails for both Tmax and Tmin, with the largest warming in the cold tail for Tmin". Klein Tank and Können (2003) indicated an increase in temperature variability due to stagnation in the warming of the cold extremes. The increase in temperatures affects the hydrological cycle and also has serious implications for natural ecosystems, human health and the economy, among others.

The DTR and vDTR indices (two measures of the difference between night and day records) had different signal trends depending on the season; for example vDTR had a negative trend in winter and autumn, but is positive in spring. The DTR index has a negative trend in winter but was positive in summer and spring. The DTR enables the changes in the maximum and minimum temperature to be interpreted to gain insights into the physical processes controlling surface temperatures (Collatz et al., 2000). Some authors state that there are seasonal differences in the DTR due to differences in cloudiness and insolation (Gallo et al., 1996; Lindvall and Svensson 2015); but the reasons for large variations in time and space are unclear (Lewis and Karoly, 2013). This study shows there is a strong seasonal relationship between radiation, cloudiness and DTR. The percentages of land with a significant positive trend in DTR, CC and SSP indices are 7%, 11%, 4% in winter, 44%, 0%, 55% in spring, 38%, 0%, 64% in summer, and 13%, 2%, 6% in autumn, respectively (Figure 11). The increase in radiation and decrease in cloudiness in summer and spring gave a positive trend in the DTR, due to the maximum temperature increase being higher than the minimum temperature (Dai et al., 1999). However, the opposite case was observed in winter with a significant positive trend across most of the land in the CC index and a small percentage in the SSp index, which led to more than two fifths of the land returning a significant negative trend in the DTR index (41%, Figure 11). Cloudiness reduces the DTR by decreasing surface solar radiation, so the minimum temperature increases more than the maximum (Dai et al., 1999). The percentage of land with a significant trend in DTR, CC and SSP indices in autumn was very low and it is not possible to obtain a clear signal. Nonetheless, the causes explaining the evolution of the DTR are not clear since there are other factors, such as vegetation, and its seasonal cycle that also strongly influences soil moisture, the fluxes of sensible and latent heat, among others affecting the DTR (Zhou et al., 2007).

As previously suggested, the trend of radiation and cloudiness is linked to the temperature trend. The temporal changes in the cloud cover alter the surface–atmosphere heating distribution, due to the dominant influence of cloud on the energy balance of the earth's climate through the cooling effect of albedo, and greenhouse warming (Sun et al., 2000). In this study, the cloud/radiation indices showed a significant trend over most of the territory in spring and summer, with a positive trend in radiation indices (SSD, SSP, and ACI), and negative in cloudiness indices (CC and FOD). Trends of all-sky downward surface solar radiation from satellite-derived data over Europe (1983–2010) show a widespread increase in across most of Europe, especially in springtime (Sanchez-Lorenzo et al., 2017). The mean annual SSR series showed an increase from the mid-1980s to the early 2000s (i.e. global brightening) mainly due to anthropogenic aerosol emissions and/or cloudiness (Wild, 2009). According to Sanchez-Lorenzo et al., (2015) the recent brightening takes place primarily in spring and summer and in the eastern and central regions of Europe, as shown in the results of this study.

Cloud cover change has a strong impact on the surface shortwave radiation (Norris and Wild, 2007), atmospheric aerosols (Norris and Wild, 2007), circulation patterns (Della-Marta et al., 2007), soil moisture and evapotranspiration (Fisher et al., 2007). In this respect, several authors (Sun et al. 2000; Tang et al., 2012) had indicated that the decreased cloud cover may have contributed to the summer warming through the effects of decrease in top-of-atmosphere reflected shortwave radiation and increase in surface shortwave radiation. Other authors (Fischer et al. 2007; Hirschi et al. 2011) had suggested that a lack of sufficient amount of soil moisture has decreased latent cooling and increased the summer maximum temperature. In this study, the strong relationship between cloudiness, solar radiation and temperature has been observed, especially in spring and summer.

The precipitation indices did not show a clear trend at seasonal scale in the study area, only the EP index (precipitation minus evapotranspiration) in summer returned a negative trend. The EP index is closely related to aridity indices, among which are ETo and CMD. The ETo index had a significant positive trend in spring and summer across most of the study area. Some authors suggest that there is increased atmospheric evaporative demand, due to a major water pressure deficit caused by higher temperatures (Wang et al 2012; Vicente-Serrano et al., 2019), resulting in more frequent and severe droughts (Dai 2011, Vicente-Serrano et al., 2014). This could cause biological stress (Williams et al 2013), reduced soil water content, runoff generation, stream flow and groundwater recharge (Cai and Cowan 2008), which would impact on water management, agriculture and aquatic ecosystems (Hisdal et al., 2001). However, the relationship between climate warming and increased atmospheric evaporative demand is the subject of scientific debate (Vicente-Serrano et al., 2019). On the other hand, the CMD index showed a north-south spatial pattern, with a positive trend in the south and a negative one in the north, especially marked in spring and summer. In this respect, Spinoni et al., (2017) indicated that drought frequency and severity showed decreasing tendencies over northern Europe, especially in winter and spring, while southern and eastern Europe showed a more significant tendency towards dryness, especially in summer and autumn, which would be explained by the evolution of the atmospheric evaporative demand (González-Hidalgo et al., 2018). In addition, Spinoni et al., (2017) pointed out that the drier conditions have recently become more prevalent over central Europe in spring, the Mediterranean area in summer, and eastern Europe in autumn. The previous results show that more severe drought, understood as the relationship between precipitation and temperature, linked to changes in the atmospheric evaporative demand, prevail in the warm season and in the south of the study area.

Otherwise, for snow, the ASD and MS indices returned a negative trend in winter and spring, and FSD and SCD only in spring. Analyzing the trend in snow data is difficult, due to the low resolution of the data against the high spatial variability of snow. Despite this, a negative trend has been observed in some snow indices that impacts on regional water resources, reduces stream flow during the growing season when demand is heaviest, thus intensifying water scarcity in dry areas, the frequency of wildfires with those at mid-elevations burning for longer, among other issues (Schlaepfer et al., 2012).

Lastly, for wind indices, a non-significant negative trend was observed on an annual scale, with no large seasonal variations. A decline in the surface wind has been recorded in various parts of the world over the past few decades, but the precise cause of the stilling is uncertain; several possible reasons include increasing land surface roughness and mesoscale circulation changes (McVicar et al., 2008; Smits et al., 2005). The wind indices used in this study were estimated from the reanalysis data, and previous studies indicated that the stilling (wind slowdown) is either not reproduced or has been largely underestimated in global reanalysis products (Vautard et al., 2010; Zeng et al., 2019). Zeng et al., (2010) indicated that the wind data showed a negative trend from 1978 to 2010, and a positive trend after 2010 on a globe scale, and specifically for Europe, the stilling reversed around 2003. This study includes both trends for the 1979-2017 period, which could have affected the significance trend. The wind trend has important implications for the values and spatial distribution of the atmospheric evaporative demand, atmospheric pollution, erosion and wind energy production, among others.

3.6 Conclusions

The analysis of the seasonal and annual trend of the 117 climate indices in Europe for the study period (1979-2017) shows general patterns according to the climate variable (category) of analysis.

The selected temperature indices show that cold days and nights had negative trends, while warm days and nights had a positive trend in most of the study territory.

For precipitation and aridity/continentality indices, the spatial coherence of the significant trends was low in the whole of the study area. Despite this, certain indices show spatial patterns, the RT precipitation index had a positive trend in northern and central areas of Europe, but in western regions it was negative. Meanwhile, the CMD aridity index showed a north-south spatial pattern, with a positive trend in the south and negative in the north, especially marked in spring and summer.

Wind indices tended toward negative trends, but these were not significant in the major part of the study area.

The cloudiness indices showed a negative trend, while a positive trend was found in radiation indices over a high percentage of the study area.

Snow indices showed a negative trend in most of the study territory, except in the coldest regions.

The analysis of the seasonal trend of climate indices showed that there are large differences between seasons, reflecting the need to conduct climate studies at different time scales in order to be able to understand the causes and consequences of climate change.

This study provides a useful tool, the ECTACI viewer, to access four statistics (climatology, coefficient of variation, slope and significant trend) from 125 climate indices for Europe at monthly, seasonal and annual scale from 1979-2017. The main advantage of the ECTACI viewer is that it enables the gridded dataset to be displayed and downloaded very intuitively, which makes it a valuable source of information for future studies. The four statistics obtained from the 125 climate indices at different temporal scales are available on the website http://ECTACI.csic.es/ maintained by the Spanish National Research Council. The ECTACI viewer may serve as a tool in several climate services, such as validation of climate models, location of wind or solar parks, indicators for health human and tourism, among others, besides helping to understand current climate change processes in Europe from a wide perspective.

3.7 Acknowledgments

This work was supported by the research projects CGL2017-82216-R and CGL2017-83866-C3-1-R and PCI2019-103631, financed by the Spanish Commission of Science and Technology and FEDER; CROSSDRO project financed by the AXIS (Assessment of Cross(X) - sectorial climate Impacts and pathways for Sustainable transformation), JPI-Climate co-funded call of the European Commission and INDECIS which is part of ERA4CS, an ERA-NET initiated by JPI Climate, and funded by FORMAS (SE), DLR (DE), BMWFW (AT), IFD (DK), MINECO (ES), ANR (FR) with co-funding by the European Union (Grant 690462). Dhais Peña-Angulo received a “Juan de la Cierva” postdoctoral contract (FJCI-2017-33652 Spanish Ministry of Economy and Competitiveness, MEC).

3.8 Data Availability Statement:

In our study we use the data from the European Climate Assessment and Dataset (ECA & D) E-OBS gridded dataset v17.0 (Cornes, R. C., van der Schrier, G., van den Besselaar, E. J. M. & Jones, P. D. 2018. An Ensemble Version of the E-OBS Temperature and Precipitation Data Sets. J. Geophys. Res. Atmos. 123, 9391–9409) and the ERA5 reanalysis database (Copernicus Climate Change Service (C3S). 2017. ERA5: Fifth generation of ECMWF atmospheric reanalyses of the global climate. Copernicus Climate Change Service Climate Data Store (CDS), date of access. **https://cds.climate.copernicus.eu/cdsapp#!/home**). In addition, we uses the “ClimInd” package (**https://cran.r-project.org/web/packages/ClimInd/index.html**) within the R platform (R Core Team, R Development Team Core, 2017. A: A Language and Environment for Statistical Computing) to compute 125 climate indices. In our study, new data is generated which is deposited in a repository that belongs to the public institution Pyrenean Institute of Ecology of the Higher Council for Scientific Research (Government of Spain) **http://ECTACI.csic.es/**.

3.9 References

Alexander, L. V., Zhang, X., Peterson, T. C., Caesar, J., Gleason, B., Tank, A. K., ... & Tagipour, A. Aguirre, (2006). Global observed changes in daily climate extremes of temperature and precipitation. *J. Geophys. Res*, 111, D05109.

Amelung, B., & Viner, D. (2006). The sustainability of tourism in the Mediterranean: exploring the future with the tourism comfort index. *Journal of Sustainable Tourism*, 14(4).

Azad, A. K., Alam, M. M., & Islam, M. R. (2010). Statistical analysis of wind gust at coastal sites of Bangladesh. *International Journal of Energy Machinery*, 3(1), 9-17.

Azorin-Molina, C., Vicente-Serrano, S. M., Sanchez-Lorenzo, A., McVicar, T. R., Morán-Tejeda, E., Revuelto, J., ... & Tomas-Burguera, M. (2015). Atmospheric evaporative demand observations, estimates and driving factors in Spain (1961–2011). *Journal of Hydrology*, 523, 262-277.

Azorin-Molina, C., Guijarro, J. A., McVicar, T. R., Vicente-Serrano, S. M., Chen, D., Jerez, S., & Espírito-Santo, F. (2016). Trends of daily peak wind gusts in Spain and Portugal, 1961–2014. *Journal of Geophysical Research: Atmospheres*, 121(3), 1059-1078.

Baltas, E. (2007). Spatial distribution of climatic indices in northern Greece. Meteorological Applications: *A journal of forecasting, practical applications, training techniques and modelling*, 14(1), 69-78.

Blazejczyk, K. (2006). Climate and bioclimate of Poland. Geographia polonica, 77, 31-48.

Bröde, P., Fiala, D., Błażejczyk, K., Holmér, I., Jendritzky, G., Kampmann, B., ... & Havenith, G. (2012). Deriving the operational procedure for the Universal Thermal Climate Index (UTCI). *International journal of biometeorology*, 56(3), 481-494.

Cai W and Cowan T 2008 Evidence of impacts from rising temperature on inflows to the Murray–Darling Basin *Geophys. Res. Lett*. 35 L07701

Chiew, F.H.S., Kamaladasa, N.N., Malano, H.M., McMahon, T.A., (1995). Penman–Monteith FAO-24 reference crop evapotranspiration and class-A pan data in Australia. *Agric. Water Manage.* 28, 9– 21

Cheng, J., Xu, Z., Zhu, R., Wang, X., Jin, L., Song, J., & Su, H. (2014). Impact of diurnal temperature range on human health: a systematic review. *International journal of biometeorology*, 58(9), 2011-2024.

Chen, D., Walther, A., Moberg, A., Jones, P., Jacobeit, J., & Lister, D. (2015). European Trend Atlas of Extreme Temperature and Precipitation Records. Springer.

Collatz, G. J., Bounoua, L., Los, S. O., Randall, D. A., Fung, I. Y., & Sellers, P. J. (2000). A mechanism for the influence of vegetation on the response of the diurnal temperature range to changing climate. *Geophysical Research Letters*, 27(20), 3381-3384.

Creed, I. F., Spargo, A. T., Jones, J. A., Buttle, J. M., Adams, M. B., Beall, F. D., ... & Green, M. B. (2014). Changing forest water yields in response to climate warming: Results from long-term experimental watershed sites across North America. *Global change biology*, 20(10), 3191-3208.

Croxford, B., Penn, A., & Hillier, B. (1996). Spatial distribution of urban pollution: civilizing urban traffic. *Science of the total environment*, 189, 3-9.

Goldie J; Alexander L; Lewis SC; Sherwood SC; Bambrick H, 2019, 'Correction to: Changes in relative fit of human heat stress indices to cardiovascular, respiratory, and renal hospitalizations across five Australian urban populations. *International Journal of Biometeorology*, (2018), 62, 3, (423-432), 10.1007/s00484-017-1451-9).

Copernicus Climate Change Service (C3S) (2017): ERA5: Fifth generation of ECMWF atmospheric reanalyses of the global climate. Copernicus Climate Change Service Climate Data Store (CDS), date of access. https://cds.climate.copernicus.eu/cdsapp#!/home

Cornes, R. C., van der Schrier, G., van den Besselaar, E. J. M. & Jones, P. D. An Ensemble Version of the E-OBS Temperature and Precipitation Data Sets. *J. Geophys. Res. Atmos*. 123, 9391–9409 (2018).

Dai A (2011) Drought under global warming: a review. *Wiley Interdiscip Rev Clim Chang* 2:45–65

Dai, A., Trenberth, K.E., Karl, T.R. (1999) "Effects of Clouds, Soil Moisture, Precipitation, and Water Vapor on Diurnal Temperature Range" *Journal of Climate* 12, 2451-2473

Della-Marta, P. M., J. Luterbacher, H. von Weissenfluh, E. Xoplaki, M. Brunet, and H. Wanner, 2007: Summer heat waves over Western Europe 1880-2003, their relationship to large-scale forcings and predictability. Climate Dyn., 29, 251–275.

Di Napoli, C., Pappenberger, F., & Cloke, H. L. (2018). Assessing heat-related health risk in Europe via the Universal Thermal Climate Index (UTCI). *International journal of biometeorology*, 62(7), 1155-1165.

Domínguez-Castro, F., Reig, F., Vicente-Serrano, S. M., Aguilar, E., Peña-Angulo, D., Noguera, I., ... & El Kenawy, A. M. (2020). A multidecadal assessment of climate indices over Europe. Scientific Data, 7(1), 1-7.

Easterling, D. R., Alexander, L. V., Mokssit, A., & Detemmerman, V. (2003). CCI/CLIVAR workshop to develop priority climate indices. *Bulletin of the American Meteorological Society*, 84(10), 1403-1407.

Easterling, D. R., Evans, J. L., Groisman, P. Y., Karl, T. R., Kunkel, K. E., & Ambenje, P. (2000). Observed variability and trends in extreme climate events: a brief review. *Bulletin of the American Meteorological Society*, 81(3), 417-426.

Falk, M. (2010). A dynamic panel data analysis of snow depth and winter tourism. *Tourism Management*, 31(6), 912-924.

Fick, S. E., & Hijmans, R. J. (2017). WorldClim 2: new 1-km spatial resolution climate surfaces for global land areas. *International journal of climatology,* 37(12), 4302-4315.

Fischer, G., Shah, M., N. Tubiello, F., & Van Velhuizen, H. (2005). Socio-economic and climate change impacts on agriculture: an integrated assessment, 1990–2080. Philosophical Transactions of the Royal Society B: *Biological Sciences*, 360(1463), 2067-2083.

Fischer, E. M., Seneviratne, S.I., Vidale, P. L., Luthi, D. & Schar, C. (2007) Soil moisture–atmosphere interactions during the 2003 European summer heat wave. J. Climate, 20, 5081–5099.

Frich, P., Alexander, L. V., Della-Marta, P. M., Gleason, B., Haylock, M., Tank, A. K., & Peterson, T. (2002). Observed coherent changes in climatic extremes during the second half of the twentieth century. *Climate research*, 19(3), 193-212.

Field, C. B., Barros, V., Stocker, T. F., Qin, D., Dokken, D. J., Ebi, K. L., ... & Tignor, M. (2012). IPCC 2012. Managing the risks of extreme events and disasters to advance climate change adaptation. A special report of the intergovernmental panel on climate change.

Fontrodona Bach, A., Van der Schrier, G., Melsen, L. A., Klein Tank, A. M. G., & Teuling, A. J. (2018). Widespread and accelerated decrease of observed mean and extreme snow depth over Europe. *Geophysical Research Letters*, 45(22), 12-312.

Gabriels, D. (2006). Assessing the Modified Fournier Index and the Precipitation Concentration Index for Some European Countries. In Soil Erosion in Europe (eds J. Boardman and J. Poesen). doi:10.1002/0470859202.ch48.

Gallo, K.P., Easterling, D.R., Peterson, T,C. (1996) “The influence of Land Use/Land Cover on Climatological Values of the Diurnal Temperature Range” *Journal of Climate* 9, 2941-2944.

Girvetz, E. H., & Zganjar, C. (2014). Dissecting indices of aridity for assessing the impacts of global climate change. *Climatic change*, 126(3-4), 469-483.

González-Hidalgo, J. C., Vicente-Serrano, S. M., Peña-Angulo, D., Salinas, C., Tomas-Burguera, M., & Beguería, S. (2018). High-resolution spatio-temporal analyses of drought episodes in the western Mediterranean basin (Spanish mainland, Iberian Peninsula). *Acta Geophysica*, 66(3), 381-392.

Haylock, M. R., & Goodess, C. M. (2004). Interannual variability of European extreme winter rainfall and links with mean large-scale circulation. *International Journal of Climatology*: A Journal of the Royal Meteorological Society, 24(6), 759-776.

Heim Jr, R. R. (2015). An overview of weather and climate extremes–Products and trends. *Weather and Climate Extremes*, 10, 1-9.

Hijmans, R. J., Cameron, S., Parra, J., Jones, P. G., Jarvis, A., & Richardson, K. (2005). WorldClim, version 1.3. University of California, Berkeley.

Hirschi, M., et al. (2011) Observational evidence for soil- moisture impact on hot extremes in southeastern Europe. Nat. Geosci., 4, 17–21.

Hisdal, H., Stahl, K., Tallaksen, L. M., & Demuth, S. (2001). Have streamflow droughts in Europe become more severe or frequent*?. International Journal of Climatology*, 21(3), 317-333.

Hoegh-Guldberg, O., Jacob, D., Taylor, M., Bindi, M., Brown, S., Camilloni, I., ... & Guiot, J. (2018). Impacts of 1.5 ºC global warming on natural and human systems. In Global Warming of 1.5° C: An IPCC Special Report on the impacts of global warming of 1.5° C above pre-industrial levels and related global greenhouse gas emission pathways, in the context of strengthening the global response to the threat of climate change, sustainable development, and efforts to eradicate poverty. IPCC.

Hong, Y. I. N., & Ying, S. U. N. (2018). Characteristics of extreme temperature and precipitation in China in 2017 based on ETCCDI indices. *Advances in Climate Change Research*, 9(4), 218-226.

Huang, S., Huang, Q., Chang, J., & Leng, G. (2016). Linkages between hydrological drought, climate indices and human activities: a case study in the Columbia River basin. *International Journal of climatology*, 36(1), 280-290.

Huang, H., Han, Y., Cao, M., Song, J., & Xiao, H. (2016). Spatial-temporal variation of aridity index of China during 1960–2013. *Advances in Meteorology*, 2016.

IPCC. Climate Change 2013: the physical science basis. Contribution of Working Group I to the fifth assessment report of the intergovernmental panel on climate change. (ed. Stocker, T.F. et al.) Cambridge University Press, United Kingdom and New York, NY, USA, 1535 pp (2013).

Karl, T.R., N. Nicholls, and A. Ghazi, 1999: CLIVAR/GCOS/WMO workshop on indices and indicators for climate extremes: Workshop summary. *Climatic Change*, 42, 3-7.

Katsanos, D., Retalis, A., Tymvios, F., & Michaelides, S. (2018). Study of extreme wet and dry periods in Cyprus using climatic indices. Atmospheric Research, 208, 88-93.

Klein Tank, A. M. G., & Können, G. P. (2003). Trends in indices of daily temperature and precipitation extremes in Europe, 1946–99. *Journal of climate*, 16(22), 3665-3680.

Klein Tank AMG, Zwiers FW, Zhang X. 2009. Guidelines on analysis of extremes in a changing climate in support of informed decisions for adaptation, climate data and monitoring WCDMP-No 72, WMO-TD No 1500, p 5.

Klok, .J. and Klein Tank, A. M. G. (2009) Updated and extended European dataset of daily climate observations. *Int. J. Climatol.* 29: 1182–1191.

Koufos, G. C., Mavromatis, T., Koundouras, S., & Jones, G. V. (2018). Response of viticulture-related climatic indices and zoning to historical and future climate conditions in Greece. *International Journal of Climatology*, 38(4), 2097-2111.

Kunkel, K.E, Robinson, D.A., Champion, S.,Yin, X., Estilow, T., Frankson, R.M. (2016) Trends and Extremes in Northern Hemisphere Snow Characteristics. *Curr Clim Change Rep* (2016) 2:65–73. DOI 10.1007/s40641-016-0036-8

Lewis, S. C., & Karoly, D. J. (2013). Evaluation of historical diurnal temperature range trends in CMIP5 models. *Journal of Climate,* 26 (22), 9077-9089.

Lindvall, J. and Svensson, G. (2015) "The diurnal temperature range in the CMIP5 models" *Clim Dyn* 44, 405-421.

McGregor, K. M., Marotz, G. A., & Whittemore, D. O. (1988). Ground water quality prediction using climatic indices. *Journal of the American Water Resources Association,* 24(1), 43-48.

Martin-Vide, J. (2004). Spatial distribution of a daily precipitation concentration index in peninsular Spain. *International Journal of Climatology,* vol. 24, no. 8, pp. 959–971.

McMichael, A. J., & Lindgren, E. (2011). Climate change: present and future risks to health, and necessary responses. *Journal of internal medicine*, 270(5), 401-413

McVicar, T. R. et al. Wind speed climatology and trends for Australia, 1975–2006: Capturing the stilling phenomenon and comparison with near-surface reanalysis output. *Geophys. Res. Lett.* 35doi:10.1029/2008GL035627 (2008).

McVicar, T. R., Roderick, M. L., Donohue, R. J., Li, L. T., Van Niel, T. G., Thomas, A., ... & Mescherskaya, A. V. (2012). Global review and synthesis of trends in observed terrestrial near-surface wind speeds: Implications for evaporation. *Journal of Hydrology*, 416, 182-205.

Moberg, A., & Jones, P. D. (2005). Trends in indices for extremes in daily temperature and precipitation in central and western Europe, 1901–99. *International Journal of Climatology: A Journal of the Royal Meteorological Society,* 25(9), 1149-1171.

Moberg, A., Jones, P. D., Lister, D., Walther, A., Brunet, M., Jacobeit, J., ... & Chen, D. (2006). Indices for daily temperature and precipitation extremes in Europe analyzed for the period 1901–2000. *Journal of Geophysical Research: Atmospheres,* 111(D22).

Moral, F. J., Paniagua, L. L., Rebollo, F. J., & García-Martín, A. (2017). Spatial analysis of the annual and seasonal aridity trends in Extremadura, southwestern Spain. *Theoretical and applied climatology,* 130(3-4), 917-932.

Nicholls, S., & Amelung, B. (2008). Climate change and tourism in northwestern Europe: Impacts and adaptation. *Tourism analysis,* 13(1), 21-31.Perch-Nielsen et al., 2010

Norris, J. R., & Wild, M. (2007). Trends in aerosol radiative effects over Europe inferred from observed cloud cover, solar ‘‘dimming,’’ and solar ‘‘brightening.’’ Geophys. Res. Lett., 112, D08214, doi:10.1029/2006JD007794.

Osczevski, R and Bluestein, M. (2005). The new wind chill equivalent temperature chart. *Bulletin of the American Meteorological Society.* 86 (10): 1453–1458

Panda, D. K., Panigrahi, P., Mohanty, S., Mohanty, R. K., & Sethi, R. R. (2016). The 20th century transitions in basic and extreme monsoon rainfall indices in India: Comparison of the ETCCDI indices. *Atmospheric Research,* 181, 220-235.

Piticar, A., Croitoru, A. E., Ciupertea, F. A., & Harpa, G. V. (2018). Recent changes in heat waves and cold waves detected based on excess heat factor and excess cold factor in Romania. *International Journal of Climatology,* 38(4), 1777-1793.

Pickering, C. (2011). Changes in demand for tourism with climate change: a case study of visitation patterns to six ski resorts in Australia. Journal of Sustainable Tourism, 19(6), 767-781.

R Core Team, R Development Team Core, 2017. R: A Language and Environment for Statistical Computing.

Rudel, E., Matzarakis, A., & Koch, E. (2007, December). Summer tourism in Austria and climate change. In MODSIM 2007 International Congress on Modelling and Simulation. Modelling and Simulation Society of Australia and New Zealand (pp. 1934-1939).

Schlaepfer, D. R., Lauenroth, W. K., & Bradford, J. B. (2012). Consequences of declining snow accumulation for water balance of mid-latitude dry regions. *Global change biology,* 18(6), 1988-1997.

Sanchez-Lorenzo, A., Calbó, J., & Martin-Vide, J. (2008). Spatial and temporal trends in sunshine duration over Western Europe (1938–2004). *Journal of Climate,* 21(22), 6089-6098.

Sanchez-Lorenzo, A., M. Wild, M. Brunetti, J. A. Guijarro, M. Z. Hakuba, J. Calbó, S. Mystakidis, and B. Bartok (2015). Reassessment and update of long-term trends in downward surface shortwave radiation over Europe (1939–2012). *J. Geophys. Res. Atmos.*, 120, 9555–9569, doi:10.1002/2015JD023321.

Sanchez-Lorenzo, A., Enriquez-Alonso, A., Wild, M., Trentmann, J., Vicente-Serrano, S. M., Sanchez-Romero, A., ... & Hakuba, M. Z. (2017). Trends in downward surface solar radiation from satellites and ground observations over Europe during 1983–2010. *Remote Sensing of Environment,* 189, 108-117.

Schlaepfer, D. R., Lauenroth, W. K., & Bradford, J. B. (2012). Consequences of declining snow accumulation for water balance of mid-latitude dry regions. *Global change biology,* 18(6), 1988-1997.

Smits, A., Klein-Tank, A. M. G. & Können, G. P. Trends in storminess over the Netherlands, 1962–2002. *Int. J. Climatol.* 25, 1331–1344 (2005).

Spinoni J, Naumann G, Vogt J. (2017). Pan-European seasonal trends and recent changes of drought frequency and severity. *Global Planet. Change* 148: 113–130.

Steadman, R.G., 1984: A Universal Scale of Apparent Temperature. *J. Climate Appl. Meteor.,* 23, 1674–1687.

Stjern, C. W., Kristjánsson, J. E., & Hansen, A. W. (2009). Global dimming and global brightening—An analysis of surface radiation and cloud cover data in northern Europe. *International Journal of Climatology: A Journal of the Royal Meteorological Society,* 29(5), 643-653.

Sun, B., Groisman, P. Y., Bradley, R. S., & Keimig, F. T. (2000). Temporal changes in the observed relationship between cloud cover and surface air temperature. *Journal of Climate,* 13(24), 4341-4357.

Tang, Q., Leng, G., & Groisman, P. Y. (2012). European hot summers associated with a reduction of cloudiness. *Journal of Climate,* 25(10), 3637-3644.

Toros, H. (2012). Spatio-temporal variation of daily extreme temperatures over Turkey. International Journal of Climatology, 32(7), 1047-1055.

Yin, H., Donat, M. G., Alexander, L. V., & Sun, Y. (2015). Multi-dataset comparison of gridded observed temperature and precipitation extremes over China*. International journal of climatology,* 35(10), 2809-2827.

Yu, G., Schwartz, Z., & Walsh, J. E. (2009). A weather-resolving index for assessing the impact of climate change on tourism related climate resources. *Climatic Change,* 95(3-4), 551-573.

Van den Besselaar, E. J. M., Klein Tank, A. M. G., & Buishand, T. A. (2013). Trends in European precipitation extremes over 1951–2010. *International Journal of Climatology,* 33(12), 2682-2689.

Vautard, R., Cattiaux, J., Yiou, P., Thépaut, J. N., & Ciais, P. (2010). Northern Hemisphere atmospheric stilling partly attributed to an increase in surface roughness. *Nature geoscience,* 3(11), 756-761.

Vincent, L. A., Aguilar, E., Saindou, M., Hassane, A. F., Jumaux, G., Roy, D., ... & Amelie, V. (2011). Observed trends in indices of daily and extreme temperature and precipitation for the countries of the western Indian Ocean, 1961–2008. *Journal of Geophysical Research: Atmospheres,* 116(D10).

Vicente-Serrano, S. M., Lopez-Moreno, J. I., Beguería, S., Lorenzo-Lacruz, J., Sanchez-Lorenzo, A., García-Ruiz, J. M., ... & Coelho, F. (2014). Evidence of increasing drought severity caused by temperature rise in southern Europe. *Environmental Research Letters,* 9(4), 044001.

Vicente-Serrano, S. M., McVicar, T. R., Miralles, D. G., Yang, Y., & Tomas-Burguera, M. (2019). Unraveling the influence of atmospheric evaporative demand on drought and its response to climate change. *Wiley Interdisciplinary Reviews: Climate Change,* e632.

Wang, K., Dickinson, R.E., Liang, S., 2012. Global atmospheric evaporative demand over land from 1973 to 2008. J. Clim. 25 (23), 8353–8361.

Williams, M., & Eggieston, S. (2017). Using indicators to explain our changing climate to policymakers and the public. *Bulletin WMO* nº, 66(2), 201.

Wild, M., Ohmura, A., Gilgen, H. & Rosenfeld, D., (2004) On the consistency of trends in radiation and temperature records and implications for the global hydrological cycle. Geophys. Res. Lett., 31, L11201, doi:10.1029/2003GL019188.

Wild, M (2005) Global dimming and brightening: A review. *Journal of geophysical research,* vol. 114, D00D16, doi:10.1029/2008JD011470, 2009.

Winkler, A.J., J.A. Cook, W.M. Kliewer, and L.A. Lider. 1974. General Viticulture. 4th ed. University of California Press, Berkeley.

Woodward, A., Smith, K. R., Campbell-Lendrum, D., Chadee, D. D., Honda, Y., Liu, Q., ... & Confalonieri, U. (2014). Climate change and health: on the latest IPCC report. The Lancet, 383(9924), 1185-1189.

Zhang, X., Alexander, L., Hegerl, G. C., Jones, P., Tank, A. K., Peterson, T. C., ... & Zwiers, F. W. (2011). Indices for monitoring changes in extremes based on daily temperature and precipitation data. *Wiley Interdisciplinary Reviews: Climate Change*, 2(6), 851-870.

Zeng, Z., Ziegler, A. D., Searchinger, T., Yang, L., Chen, A., Ju, K., ... & Liu, J. (2019). A reversal in global terrestrial stilling and its implications for wind energy production. *Nature Climate Change,* 9(12), 979-985.

Zhou, L., et al (2007) Impact of vegetation removal and soil aridation on diurnal temperature range in a semiarid region. P. Natl. Acad. Sci. 13, 17937-17942.